Atomistic Energetics and Critical Twinning Stress Prediction in Face and Body Centered Cubic Metals: Recent Progress

Piyas Chowdhury
Department of Mechanical
Science and Engineering,
University of Illinois at Urbana-Champaign,
1206 W. Green Street,
Urbana, IL 61801

Huseyin Sehitoglu[1]
Department of Mechanical
Science and Engineering,
University of Illinois at Urbana-Champaign,
1206 W. Green Street,
Urbana, IL 61801
e-mail: huseyin@illinois.edu

This paper recounts recent advances on the atomistic modeling of twinning in body-centered cubic (bcc) and face-centered cubic (fcc) alloy. Specifically, we have reviewed: (i) the experimental evidence of twinning-dominated deformation in single- and multi-grain microstructures, (ii) calculation of generalized planar fault energy (GPFE) landscapes, and (iii) the prediction of critical friction stresses to initiate twinning-governed plasticity (e.g., twin nucleation, twin–slip and twin–twin interactions). Possible avenues for further research are outlined. [DOI: 10.1115/1.4038673]

1 Introduction

Formation of various defects (e.g., slip, twin) and their interactions with interfaces constitute the microscopic deformation scenario [1]. At the atomic level, the stacking fault energy landscape (also known as the γ surface) is a crucial signature of a specific fault nucleation. It is suggested that the exact nature of the γ energy surface would dictate the initiation of a specific defect (i.e., slip or twinning) at the elasto-plastic juncture [2–5]. The exact magnitude of this important energetic parameter is a function of the extent of solid solution, solute segregation, and volumetric misfit among atoms of different chemical species. Recent studies have noted interesting utilization of the γ surface in formulating critical resolved shear stresses for twinning in face-centered cubic (fcc) and body-centered cubic (bcc) alloys. The phenomenon of twinning is of paramount importance due to the associated enhanced toughening attributes as manifested in experiments [6–8].

Significant physical contribution to the micromechanism of deformation originates from the discrete lattice-scale governing principles [9,10]. At continuum length scale, the current description of deformation mechanics is of phenomenological nature [11–13]. At the smallest length scale, however, the material building blocks consist of discrete atoms. The laws of interatomic interactions are drastically different from the continuum laws suitable for describing bulk materials behaviors. The atomic-level deformation scenario is governed by the Schrodinger's equation [14] addressing electronic structure while the laboratory-scale deformation is best captured by empirical elasto-plastic laws. Despite the apparent dissimilarity among these largely spanned physical length scales, subtle effects at the atomic scale would reverberate across the length scales, eventually contributing toward the observed continuum-scale mechanical behaviors [2]. For instance, the fault energetics is subjected to addition of certain solute types, which would essentially modify the energies from the base metal levels [3–5]. This in turn would alter what defect mechanism would be predominant (such as slip versus twinning) during the early plastic deformation periods. In particular, the defect formation propensity at the elasto-plastic juncture is crucial, in that the subsequent evolution of plasticity would be largely controlled by the predominant defects. The outcomes of mesoscopic plastic events would eventually decide the exact nature of the macroscale constitutive behaviors. Thus, establishing the energy landscape is an important step in the physical understanding of the alloy plastic behavior. The physical mechanisms of deformations (e.g., slip, twinning) can be qualitatively studied through atomic-scale simulations. Moreover, the quantification of intrinsic defect generation can be elucidated from atomistically based methods [15,16].

From a modeling perspective, it has long remained a challenging task to transition from atomic scales to meso- or to a higher length scale [17,18]. Consideration of atomic phenomena in modeling is nontrivial, in that the propensity to seek the energetic ground state at the lattice scale dictates the exact nature of nucleated defects during plastic deformation (i.e., slip or twinning). Nonetheless, such theoretical efforts are compounded by the requirement of high computational capacity to simulate the mesoscale phenomena. Microscopically, there are the consideration of material interfaces being intercepted by other propagating defects (such as twin and/or slip) [19–21] to a gradually increasing degree. The specific nature of the interception mechanism, and their relative predominance, essentially plays a major role in the local deformation on a grain by grain basis. For example, dislocation transmission [22,23], lock formation [24,25], incorporation into boundaries [26,27], and dislocation multiplication [28] at the interfaces constitute some of the most significant interactions that can physically occur. The energetic scenario of these physical mechanisms, if extracted accurately, can provide a sound basis for understanding their relative predilections. Depending on the boundary type, texture, etc., certain reactions may be preferred. However, the γ surface can serve as a unique signature for a certain plastic mechanism in a pristine crystal setting. The two most widely used simulation methods to study the foregoing problems are molecular dynamics and density functional theory (DFT). Interested readers are referred to the text books by Tadmor and Miller [14] and Frenkel and Smit [29], which narrate the particulars of these modeling methods.

To develop an in-depth understanding of such small length scale phenomena, today one needs a synergy of experimental study and computer simulations. For example, the changes in microstructure due to deformation are manifested as strain gradients, which can be detected with experimental techniques. The predominant defect types can then be studied with advanced digital image correlation (DIC), transmission electron microscopy (TEM), and scanning electron microscopy (SEM), and electron backscatter diffraction (EBSD). These experimental characterizations can form the basis

---

of modeling. In the paper, we begin with examples on Co-Ni and Fe-Cr alloys on the modeling ground; we will extensively discuss the use of the γ energetics concepts to rationalize twinning phenomena. In that regard, it is important to note here that comprehensive reviews related to deformation twinning are duly recorded in the literature. For example, the survey by Christian and Mahajan [30] deals with experimental behaviors and phenomenological theories. More recently, review works by Beyerlein et al. [31] and Zhu et al. [32] describe the mechanisms of twinning in the nanocrystalline microstructure. In the current paper, we discuss only the mechanistic aspects related to the discrete lattice energetics. Overall, we envision that superior predictive capabilities useful for industrial-level applications would ultimately emerge through the sequential multiscale studies, which combine atomic-scale physics with meso-scale phenomenology (Fig. 1).

The paper is organized as follows: In Sec. 2, we briefly overview some latest experimental characterization results, which reveal twinning-mediated plasticity in representative alloys. Then, we summarily critique historically important models in Sec. 3, and how these models motivated further refinement. Section 4 introduces the concept of the atomistic fault energetics and its significance in the metal plasticity. In Sec. 5, we first overview historical models for predicting twinning stress, and then describe the latest stress-prediction schemes utilizing fault energetics. The topic of annealing twins, their roles in slip transfer, extension of energetic models in mechanistically interpreting plastic flow and predicting critical stresses are discussed in Sec. 6. In Sec. 7, we outline potential avenues of further research, which are emerging alongside the current topics such as polycrystalline deformation, fracture mechanism, hexagonal close packed (hcp) deformation, and phase transformation. We conclude in Sec. 8 by commenting on the proper use of atomistics in further research and their potential usefulness in understanding larger length scale plastic deformation.

2   Brief Discussion of Experimental Results

This section contains a brief overview of recent experimental findings on the deformation behavior of: (a) single crystals and polycrystals of bcc Fe-47.8%Cr (atomic), (b) single crystals of fcc Co-33%Ni alloys, and (c) polycrystals of Ni-x%Co alloys of various Co contents (where $x = 1$, 1.62, 2.9, and 5.6). The reason for selecting these case studies for discussion is that comprehensive atomistic modeling has also been undertaken on the same materials. Hereafter, we refer to the materials as Fe-Cr, Co-Ni, and Ni-Co alloys, respectively.

2.1 Deformation of Co-Ni Single Crystals and Nanotwinned Ni-Co Polycrystals. In Fig. 2(a), the single-crystal Co-Ni alloys of fcc crystal structure are deformed in tension along $\langle 111 \rangle$ direction. The stress–strain response up to a resolved strain level of 1%
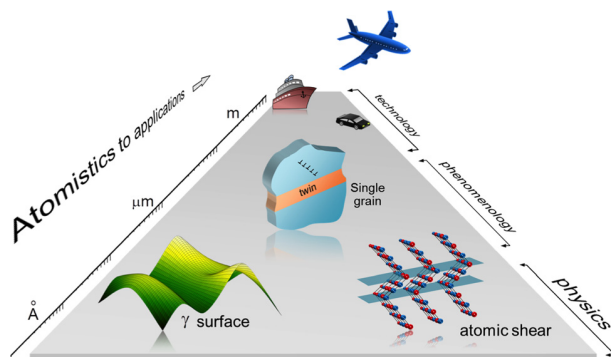

Fig. 1   A perspective on the goal of using atomistics to develop physically based theories that can capture the phenomenology of deformation, and thus formulate strategies for property enhancement in novel alloys of wide technological importance

is shown. Low-resolution DIC measurement conducted in situ shows noninteracting parallel strain bands corresponding to $(1\bar{1}1)[121]$ twin system. This system experienced the maximum Schmid factor of 0.47. The EBSD scan indicates a crystal misorientation of 60 deg between the strain band and the matrix material (i.e., suggestive of twinning). The TEM micrographs further confirm the presence of nanoscale deformation twins. Throughout the deformation range, additional parallel and noninteracting twins nucleate. These twins propagate and intercept slip substructure, resulting in the twin migration process. No twin–twin interaction is observed up to a resolved strain level of 1%. It should be noted that at higher strain, the secondary systems are likely to activate, resulting in more complex strain band patterns.

Similar observations are made for the specimens compressed along $\langle 001 \rangle$ direction as in Fig. 2(b). The (resolved) stress–strain curve along with the microstructure characterization (via DIC, EBSD and TEM) is presented. The single crystal under $\langle 001 \rangle$ compression deforms predominantly via twinning. In another case, postdeformation microstructures of $\langle 123 \rangle$ tension and $\langle 111 \rangle$ compression case unveil a plastic mechanism dominated entirely by slip on the maximum Schmid factor system (not shown). In other words, either slip or twinning is triggered only when the maximum resolved shear stress for either system is reached.

Figure 2(c) presents the differences in the stress–strain responses for four compositions of Ni-Co alloys (with 1%, 1.62%, 2.9%, and 5.52% Co contents) [33]. The microstructure of each alloy is characterized by a significant presence of annealing twins (unlike the Co-Ni cases, which experienced nucleation of twins during deformation). The deformed microstructure of the Ni-2.9%Co shows a build-up of slip around the twin boundaries as the TEM image shows. Despite very similar microstructure (in terms of twin and grain distributions), their plastic strengths, however, show a nonuniform trend with respect to Co content. The flow stress increases from 1%Co to 2.9%Co and then drops for the case of 5.52%Co. As we will discuss in Sec. 4, the physical origin of twinning-dominated plasticity in Co-Ni alloys, the composition effects in Ni-Co alloys, etc., can be rationalized in the light of alloying-induced fault energy surfaces.

2.2 Deformation of Fe-Cr Single Crystals and Polycrystals. As in Fig. 3(a), during tension along $[0\bar{1}0]$ direction, the single crystal first undergoes slip nucleation on the $[\bar{1}11](121)$ system [34]. The critical resolved shear stress, $\tau_{\text{CRSS}}^{\text{slip}}$, for the active slip system was determined to be 85 MPa. An abrupt load drop was noted marking the point where twin nucleation occurs. The critical resolved shear stress for twin nucleation $\tau_{\text{CRSS}}^{\text{twin}}$ was measured to be 177 MPa. By determining the possible systems with the maximum Schmid factors, the interacting strain bands (in SEM and DIC images) are identified as the twinning systems: $[11\bar{1}](12\bar{1})$ and $[11\bar{1}](\bar{1}21)$. The further confirmation of the strain bands of the $\langle 111 \rangle(121)$ type twins is obtained from the EBSD scan. Subsequent rise in the flow stress leads to the twin migration process (i.e., slip or another twin intercepting the previous twin).

Similarly, for the $[101]$ compression, the slip nucleation occurs at $\tau_{\text{CRSS}}^{\text{slip}} = 87$ MPa and the twin nucleation at $\tau_{\text{CRSS}}^{\text{twin}} = 202$ MPa as in Fig. 4. Prior to the initiation of twinning, there exists a flow stress plateau, which is presumably caused by a significant build-up of the slip localization, a precursor to the twinning process. This inference is supported by the DIC observation that a greater distribution of localized strain is noted for $[101]$ compression. The active slip systems were determined as $[1\bar{1}1](121)$ type (not shown). Following substantial amount of slip accumulation, twinning shear bands are found to have nucleated as the $[1\bar{1}1](121)$ and $[1\bar{1}1](1\bar{2}1)$ types.

The stress–strain response of the polycrystalline Fe-Cr alloys is presented in Fig. 3(c) [35]. No flow stress drop occurs in this case. The DIC image demonstrates considerable degree of local straining in the form of noninteracting parallel bands (caused by slip) in individual grains. The strain bands are deflected at the grain boundaries. The suppression of twinning is presumably facilitated by
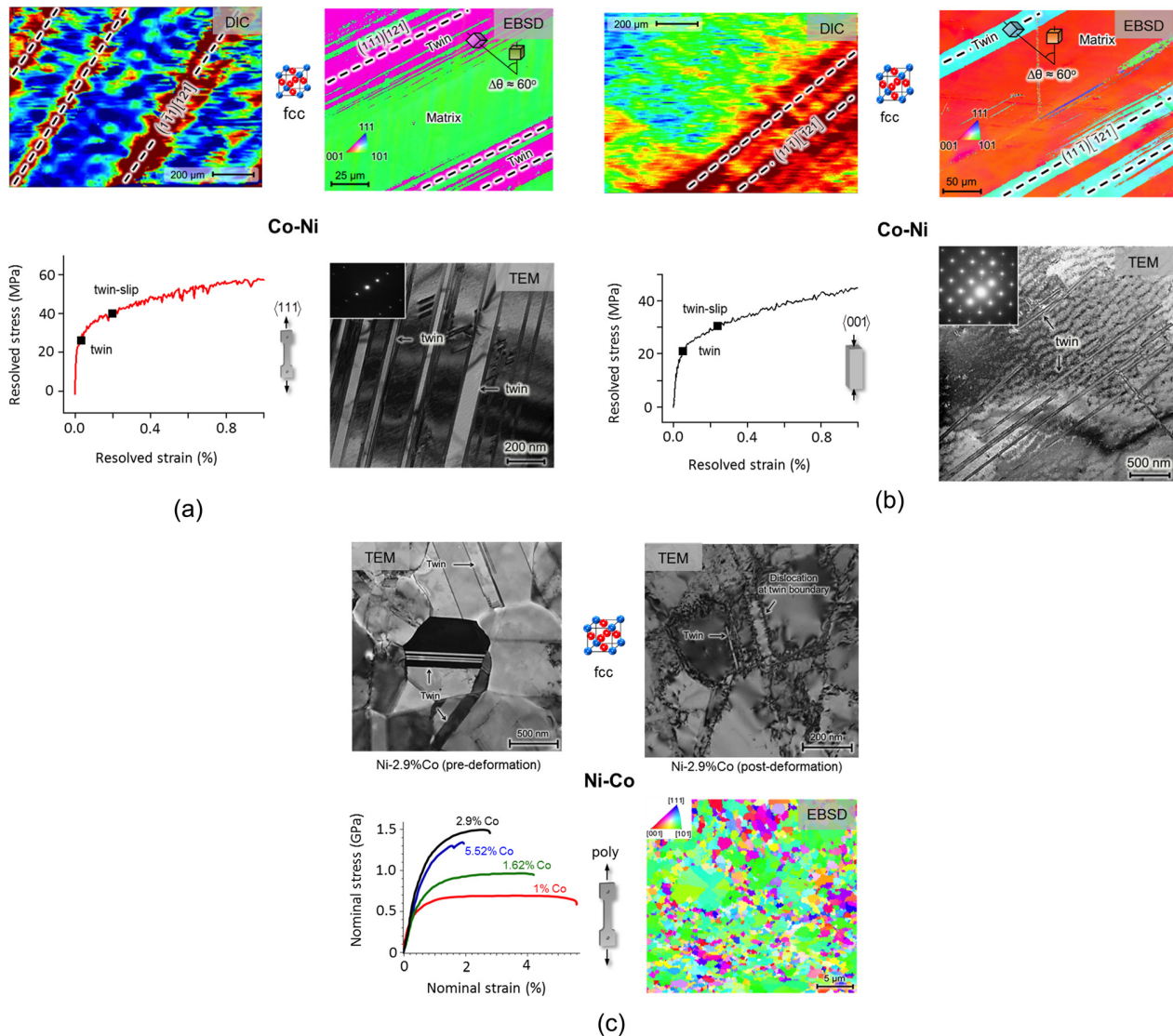
Fig. 2 (*a*) The Co-Ni crystal under ⟨111⟩ tension plastically deforms predominantly via twinning and twin-slip interactions as confirmed by DIC, EBSD, and TEM [52]. (*b*) Co-Ni compressed along the ⟨001⟩ orientation demonstrates parallel twinning as the primary deformation mechanism [52]. (*c*) The deformation of electrodeposited nanocrystalline (as indicated by EBSD analysis) Ni-Co alloys with pre-existent annealing twins shows a strong composition effect [52]. The deformation behavior is found to be characterized by massive slip–twin boundary interactions via electron microscopy.

the presence of grain boundaries. It is worth recalling that higher resolution images are typically required for resolving strains for polycrystalline microstructure. This is because the primary purpose is to determine how strain transfer occurs at the grain boundaries. To that end, a large area of interest spanning several grains was selected for DIC measurement, which in turn required very high resolution ex situ measurement. On the other hand, the strain bands can be detected with more ease in single crystals with relatively small resolution. The DIC images for the Fe-Cr polycrystal in Fig. 2(*c*) are performed ex situ by digitally stitching 140 correlated images to accurately map the strain contours. Such precision was not employed for the case in Fig. 2(*a*), where only one image (per load step) is analyzed to detect the presence of strain bands.

3 Brief Overview of Classical Mechanistic Models of Twin Nucleation

3.1 Pole Mechanism (bcc). Cottrell and Bilby [36] originally envisioned the formation of an embryonic mechanical twin in bcc lattice via the so-called pole mechanism. Figure 5 illustrates the

mechanism leading to a three-layer twin nucleation. Triggered by applied loads, a perfect dislocation of the type $(a/2)[111]$ lying on the $(11\bar{2})$ plane dissociates into two dislocations: $(a/3)[112]$ and $(a/6)[11\bar{1}]$. The dislocation $(a/3)[112]$ is a sessile one of pure edge type, and acts as an anchor, i.e., the so-called pole on the $(11\bar{2})$ plane. The partial dislocation $(a/6)[11\bar{1}]$ moves away from the pole, i.e., bows out and creates a plane of stacking fault (gray portion), which is co-planar with the pole. Since the $(a/6)[11\bar{1}]$ dislocation is curved, it would have segments consisting of pure screw type. The pure screw portion of the expanding loop cross-slips into another {112}-type plane, i.e., $(\bar{1}21)$ or $(2\bar{1}1)$. The cross-glided partial sweeps around the pole, and thus creates a monolayer stacking fault. This sweeping dislocation climbs into the adjacent parallel plane, and sweeps around the pole to create the second layer of stacking fault. In the process, the twining partial bypasses the previous layer by a separation distance of $a/\sqrt{6}$. Under continued applied loads, the twinning dislocation spiral upwards, and in the process adds more layers to the initial one.

The expression for the critical twin nucleation stress based on the pole mechanism is: $\tau_{\text{CRSS}}^{\text{twin}} = \gamma_{\text{us}}/b$, where the γ_{us} is the unstable
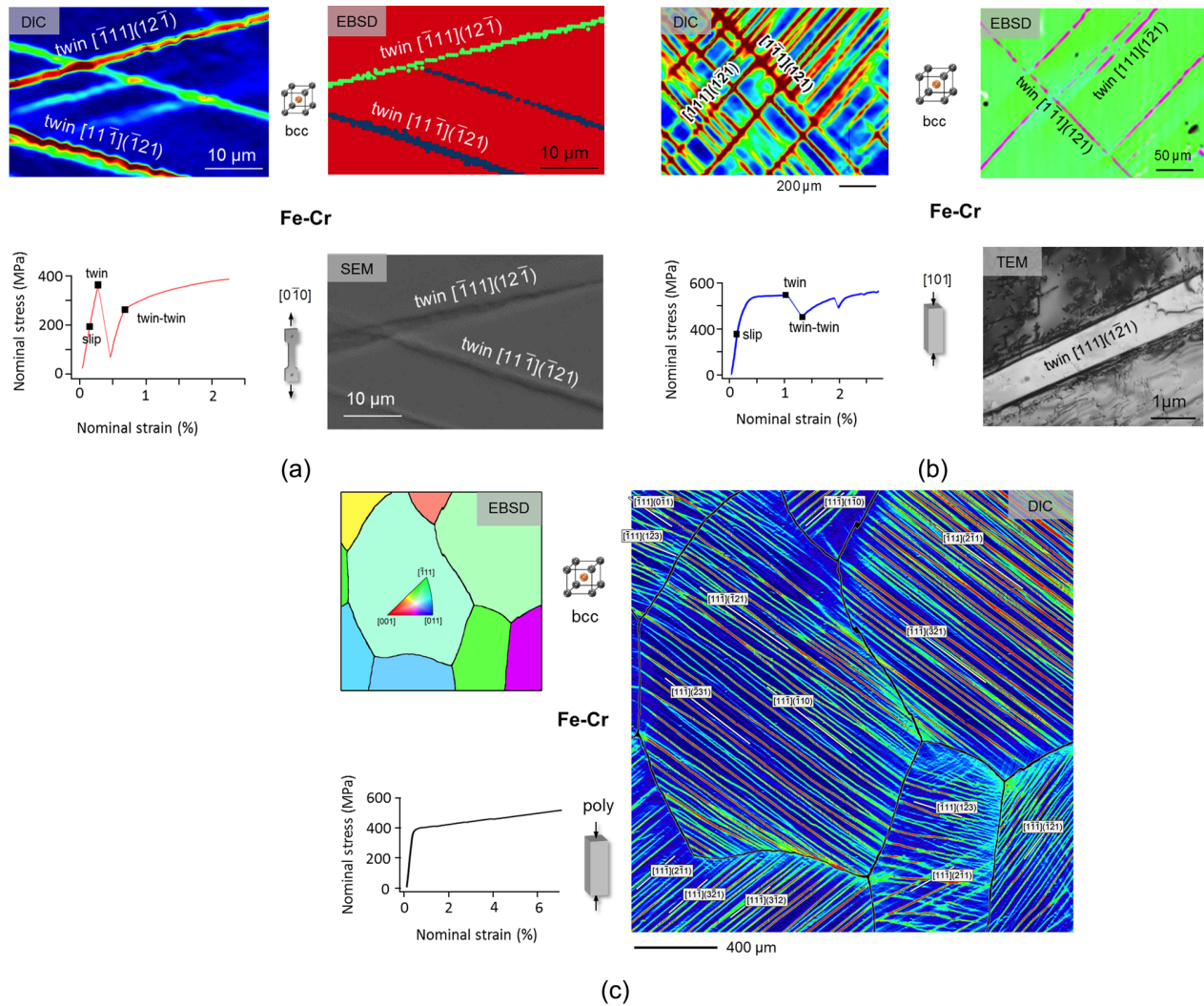
Fig. 3 (*a*) Fe-Cr single crystal under $[0\bar{1}0]$ tension deforms via interacting deformation twins as evidenced in DIC, EBSD, and SEM analyses [34]. (*b*) The deformation mechanism of Fe-Cr single crystal under $[101]$ begins with slip activities followed by twin nucleation, which causes a stress drop [34]. Subsequently, twin–twin interactions give rise to hardening as substantiated by DIC, EBSD, and TEM techniques. (*c*) Polycrystalline Fe-Cr stress–strain response is found to be governed by massive strain transfer across grain boundaries [35] (as confirmed by combined EBSD and DIC studies).

stacking fault energy (maximum energy in generalized stacking fault energy (GSFE) curve). For example, using γ_{us} magnitude of 617 mJ/m^2 [37] for pure bcc Fe, the τ_{CRSS}^{twin} is found to be 7050 MPa, which is considerably higher than the experimentally determined value of 170 MPa [38]. In other words, the stress required to operate the pole mechanism is very large. As a result, the occurrence of pole mechanism is very unlikely to occur in reality, and has never been substantiated experimentally. The underlying reason is related with the requirement monolayer stacking fault formation. The creation of a monolayer stacking fault is unlikely owing to very high magnitude of stacking fault energy in the bcc lattice (e.g., 593 mJ/m^2 for pure ferritic Fe). Furthermore, due to uni-directional nature of twinning shear [39], the roundabout sweep of the partial around the pole would also require overcoming very high energy barrier encountered in the so-called anti-twinning direction [30].

3.2 Core Dissociation Model (bcc). The dissociation of a pure screw dislocation core ultimately leading to the twin formation was first proposed by Lagerlöf [40] and Sleeswyk [41]. Figure 6 illustrates the process. Due to the instability of the nonplanar core, a screw dislocation of $(a/2)\langle111\rangle$ type can dissociate into three $(a/6)\langle111\rangle$ fractional ones on the nonparallel $\{112\}$ planes. Such a configuration is stable without any applied stress. However, when the applied mechanical forces are sufficiently large, two of the fractional dislocations tend to glide to the most stressed $\{112\}$ plane. Thus, two $(a/6)\langle111\rangle$ dislocations eventually cross-slip onto the planes parallel to the one containing the third dislocation. Continuation of applied loading results in the further gliding away of theses dislocations in the same direction, generating the adjoining stacking faults. These stacking faults separated only by one atomic layer constitute a twin embryo. The concept of twin nucleation as a result of slip dissociation is also discussed by Ogawa [42] and Priestner and Leslie [43]. From the dislocation core dissociation mechanism, τ_{CRSS}^{twin} is proposed to be $3\gamma_{isf}/b$. Using $\gamma_{isf}=$ 593 mJ/m^2 for pure Fe, τ_{CRSS}^{twin} is estimated to be 2500 MPa for bcc Fe (compare this with the experimentally found magnitude of 170 MPa). As a result, this mechanism is also very unlikely to occur in real materials.

3.3 Pole Mechanism (fcc). While it is quite improbable that the single pole-based mechanism would ever transpire in bcc lattice, the fcc crystals with relatively low γ_{isf} are known for having
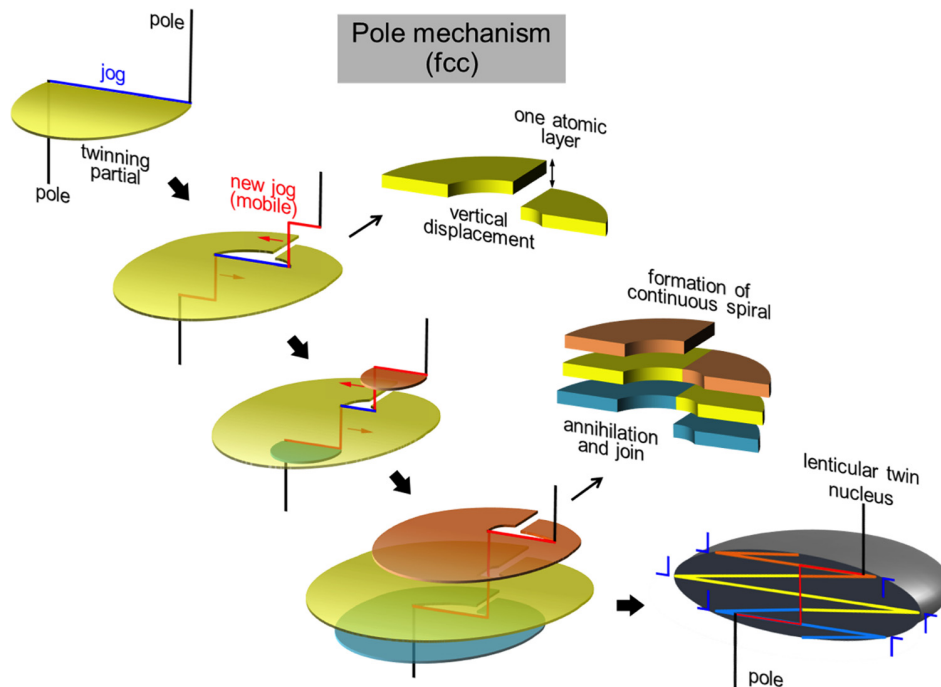
Fig. 4 Nucleation of a twin embryo through the pole mechanism in fcc lattice is proposed to be controlled by a simultaneous process of mobile jog formation and dislocation loop expansion [44–46]. Expanding slip loops from two adjoining planes eventually interconnect to form a continuous spiral, ultimately leading to the twin nucleation.
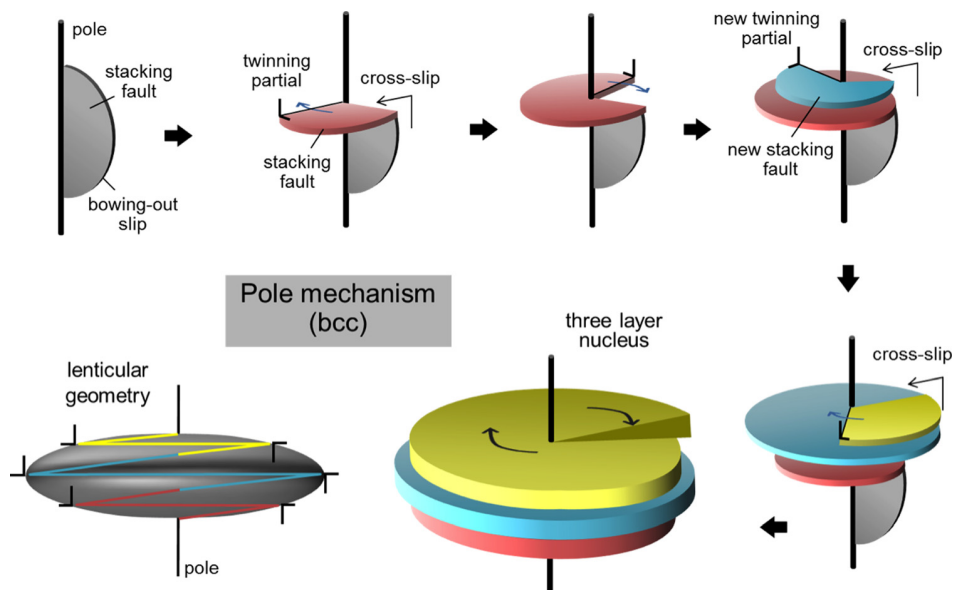

Fig. 5 An illustration of twin nucleation model via pole mechanism in bcc lattice [30,36]. An expanding slip loop stemming from sessile dislocation (pole) cross-slips into a perpendicular plane. Subsequently, the dislocation continues to revolve around the pole assisted by further cross-slips and hence generates layers of stacking faults, i.e., the twin embryo.

stable monolayer stacking faults. Modified versions for the pole-induced twinning process are proposed by Venables [44,45] and Sleeswyk [46] as illustrated in Fig. 4.

At the outset, there exists a pole dislocation with a long jog from which a loop of Shockley partial of type $(a/6)\langle 112 \rangle$ emits on a $\{111\}$ plane. With applied loading, the expanding glissile partials sweep around the two poles. Due to the sweeping at two poles, portions of the expanding loop come in the close vicinity.

In addition, at the same time, two new jogs are created at both poles. The meeting ends of the sweeping partial do not intercept head-on; rather a vertical displacement of one atomic layer occurs during the glide. Meanwhile, the newly created mobile jogs serve as two new sources for two more Shockley partials in one atomic layer below and above the first one. With moving jogs (toward each other), new twining dislocations expand, and undergo a similar wrap-around the pole followed by an offset of atomic layer.
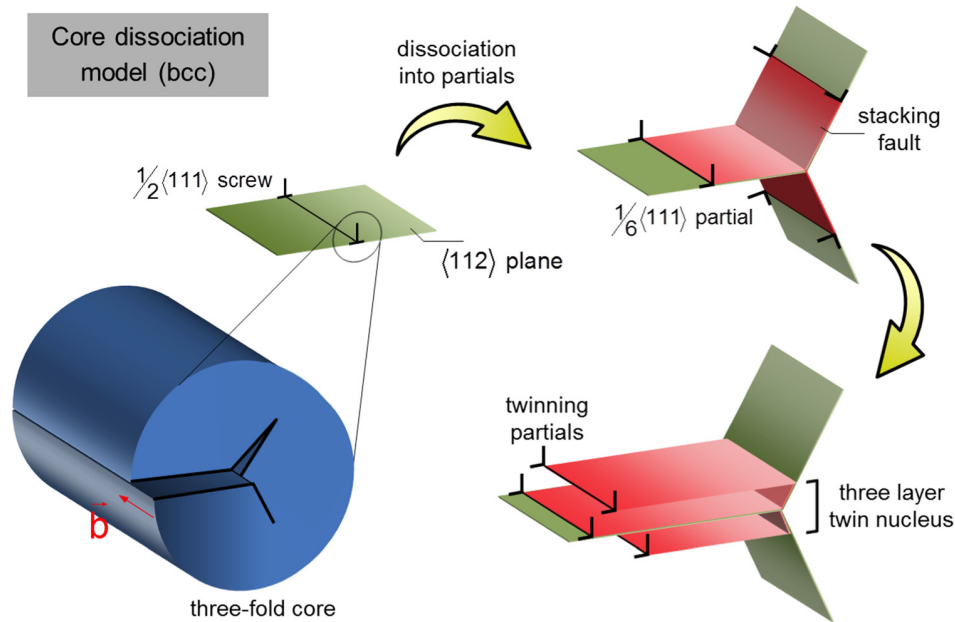
Fig. 6 The dissociation of a screw dislocation with three-fold core in bcc materials into three fraction dislocations under applied stress [40–43]. Two of the fractional dislocations (the most stress ones) cross-glide and become parallel to the third one, thereby forming a three-layer twin nucleus.

Now, one partial annihilates another loop, thus joining different layers of stacking fault, forming a continuous spiral. With three adjoining fault layers, a twin nucleus is formed.

3.4 Fault Pair Model (fcc). Noting the experimental evidence of significant pretwinning slip activities, Mahajan and Chin [47] proposed that deformation twins in fcc lattice would nucleate due to the interaction between fault pairs (also known as extrinsic stacking fault). Figure 7 describes a simplified version of the model. Due to low γ_{isf}, two full dislocations of $(a/2)\langle 110 \rangle$ type dissociate into two pairs of Shockley partials separated by ribbons of stacking fault on the same $\{111\}$ twinning (or slip) plane. Interaction with other pairs of similar extended dislocations from the adjacent layer leads to the creation of two extrinsic stacking faults (i.e., two adjoining stacking fault layers). Under continued applied stress, two such fault pairs further interact with each other, whereupon mutual annihilation as well as further cross-glide results in three consecutive layers of fault planes. This assembly constitutes a twin embryo.

3.5 Atomistic Shear Model (fcc and bcc). Layer-by-layer accumulation of stacking faults is the key to theorizing the twinning process. Such phenomenon would essentially be subjected to overcoming fault energy landscape from the discrete crystal level. As Fig. 8 illustrates, the formation of an embryonic twin in a metallic lattice would encompass rigid shearing of the parent crystal (matrix), leading to the mirrored atomic arrangement. This process is aided by glissile twinning partials [48,49].

Classically, the most important crystal-related parameter associated with twinning has been the γ_{isf}. It has been regarded for a long time that the increased twinning propensity is associated with a low γ_{isf}, for example, in fcc metals and alloys. As a result in the classical phenomenological literature [50], the parameter γ_{isf} has been used extensively as the twinnability assessment metric. However, the most recent experimental findings suggest that the γ_{isf} alone cannot fully interpret the competition between the slip versus twinning. As demonstrated in Fe-Cr and Co-Ni single crystals, the fact that either mechanism is initiated only by the maximum resolved shear stress (by varying loading/crystallographic directions) implies that the respective energy barriers

must be of comparable magnitudes. To seek the answer to these experimental discoveries, theoretical calculations of twinning stresses are conducted using the γ surface first introduced by Vitek [51].
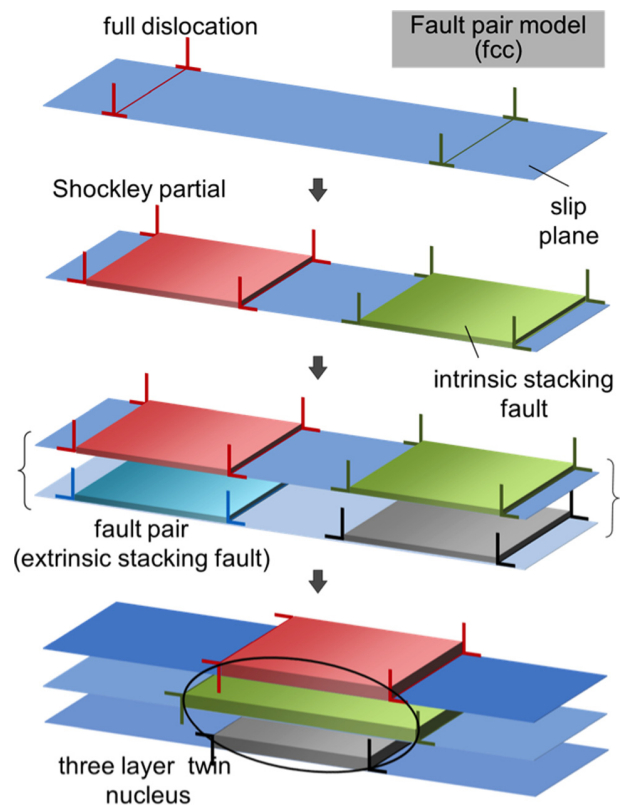

Fig. 7 Full dislocations dissociate into partials connected by intrinsic stacking faults [47]. Two extended dislocations from adjoining planes form a two-layer fault, i.e., an extrinsic stacking fault. Interaction between two extrinsic stacking faults leads ultimately to twin formation.
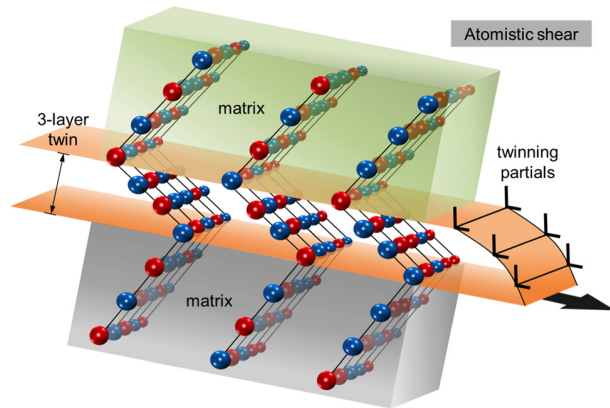
Fig. 8 The atomistic configuration of a deformation twin produced from lattice shearing induced by consecutive glide of slip [52]

4 Atomistic Fault Energetics of Slip and Twinning

4.1 Generalized Stacking Fault Energy (GSFE) or γ Surface. Figure 9 illustrates a cutaway view of a single slip plane from the {111} family in an fcc lattice along with the calculated γ surface for fcc Ni-2.9%Co [52] from DFT simulations. Such energy landscape can be computed from embedded atom method (EAM) based on molecular statics simulations as well. It is generally known that the DFT methods produce more accurate results. The accuracy of the EAM based calculations is a function of the relaxation schemes (e.g., full relaxation, vertical relaxation, and volume relaxation) and potential itself. For example, a comparison of DFT versus EMA-based predictions is performed by Chowdhury et al. [33] considering the role of composition on the intrinsic stacking fault energy in fcc Ni-Co alloys. The γ_{isf} value of pure Ni was predicted to be about 128 mJm^{-2} both from DFT [53] and EAM formalism [54]. However, DFT-predicted values for Ni-Co alloys differ significantly from the EAM values computed using two different potentials: by Zhou et al. [54] by Pun and Mishin [55].

The physical significance of such energy landscape is related with intrinsic material preference to follow the minimum energy

path for lattice shearing [56]. These energy descriptions are important indicators of the competition among full/partial slip and mechanical twinning. In an fcc lattice, to calculate the entire energy landscape, two adjoining crystal blocks are rigidly sheared by an incremental displacement of $\mathbf{u} = \mathbf{u}_{\langle 110 \rangle} + \mathbf{u}_{\langle 112 \rangle}$. For a full dislocation of $(a/2)\langle 110 \rangle$ type, the shear displacement, $\mathbf{u}_{\langle 110 \rangle}$, is imposed between the two blocks. On the other hand, for a Shockley dislocation of type $(a/6)\langle 112 \rangle$, the crystal is rigidly sheared along a $\langle 112 \rangle$ direction by the displacement vector, $\mathbf{u}_{\langle 112 \rangle}$. The preference of $(a/2)\langle 110 \rangle$ slip over $(a/6)\langle 112 \rangle$ slip can be predicted from comparing the respective peak energies [57]. The GSFE profile presented in Fig. 10 represents an energy–displacement relationship for an extended dislocation in Co-33%Ni [52].

4.2 Generalized Planar Fault Energy. The generalized planar fault energy (GPFE) is the energy–displacement curve, which is created upon layer-by-layer shear displacement of atomic blocks [3,57]. In Fig. 11(b), the GPFE for the Co-Ni is presented as an example. Starting from a perfect fcc stacking, an intrinsic stacking fault (corresponding to an energy γ_{isf}) is first created by the shearing the crystal by one Burgers vector. The energy barrier to overcome the creation of the stacking fault is designated as the γ_{us} (the so-called unstable stacking fault energy). The energy profile up to this point in fact corresponds to that of the GSFE. However, unlike the GSFE construction, the subsequent rigid shear (after one Burgers vector of displacement along a certain plane) is conducted on an adjacent parallel plane, which is one atomic layer above. The displacement of one Burgers vector in the neighboring layer forms a two-layer fault, which is also known as "the extrinsic stacking fault." The shear displacement by the same amount on the third consecutive layer produces a twin nucleus. Further displacement of adjoining planes adds more layers to the twin embryo, which is known as the twin migration process.

Figure 11(c) presents both the GSFE and GPFE curves for pure bcc Fe and Fe-50%Cr materials for a $\langle 111 \rangle \{112\}$ system. The energy barrier to slip (from GSFE) is considerably higher than that of twinning. However, unlike fcc twinning, bcc materials are characterized by either perfectly reflective twin or the so-called isosceles twin (which can be understood as a reflective atomic arrangement, however, slightly displaced along the boundary). It was discovered from the atomistic calculations that in pure bcc
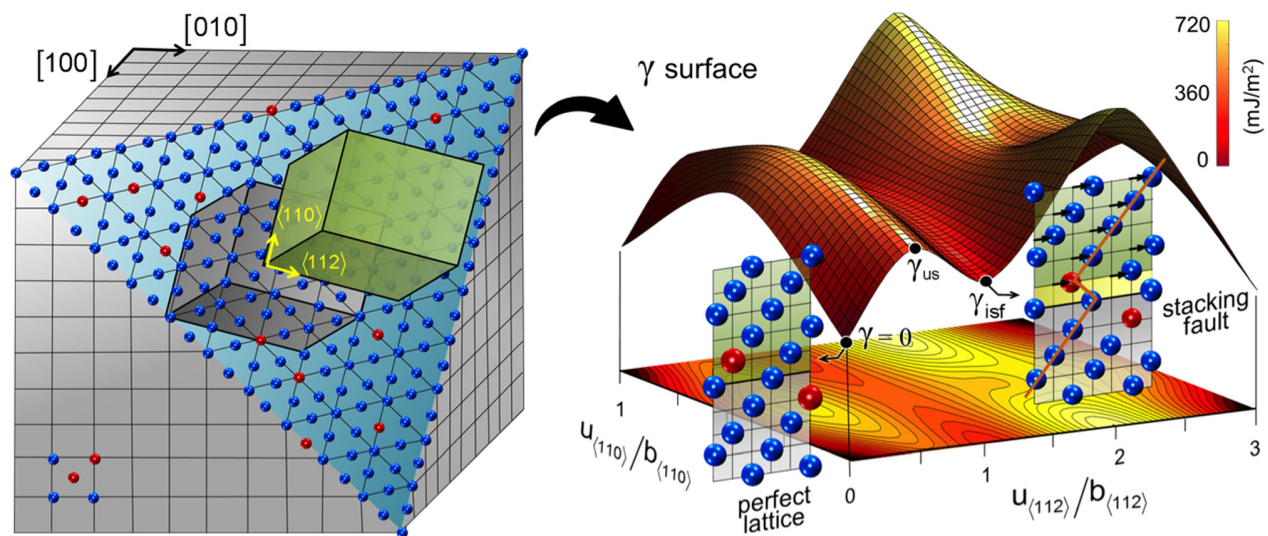

Fig. 9 To generate a γ surface, crystal blocks consisting of atoms are rigidly sheared in atomic simulations. The atomic structures of the perfect lattice and the one corresponding to an intrinsic stacking fault are shown [52] as computed from DFT simulations.
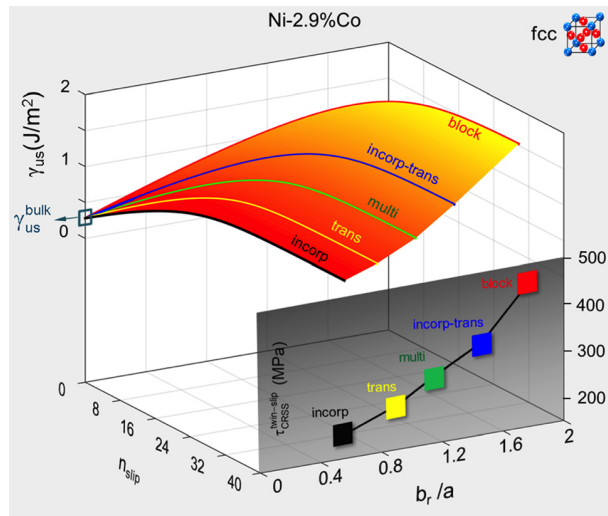
Journal of Engineering Materials and Technology

APRIL 2018, Vol. 140 **/ 020801-7**

Fig. 10 Evolution of energy barriers for various slip–twin interaction mechanisms with respect to the number of incident slip (n_{slip}) and the predicted frictional stresses ($\tau_{\text{CRSS}}^{\text{twin−slip}}$) [105]

Fe, the isosceles boundary corresponds to the minimum energy path while the reflective one is favored in the Fe-50%Cr.

**4.3 Generalized Stacking Fault Energy/Generalized Planar Fault Energy as Indicators for Preferred Deformation Mechanism.** The relative shapes of the GSFE and GPFE curves could be used as a general indicator of which deformation mode would be favored in a pristine crystal, i.e., free of grain boundaries, texture, or any other source of local stress concentration [57–59]. A definitive description of deformation trend could be more physically rationalized by comparing the γ landscapes [3,60]. Figure 12(a) illustrates various energy scenarios and their implications regarding the defect nucleation propensity in pristine fcc crystals. For the convenience of comparison, let us consider three hypothetical cases with the same magnitude of the γ_{us} but varying γ_{isf} and γ_{ut}. In a case where the γ_{isf} is considerably low and γ_{ut} is high, the plastic deformation would be characterized by dissociated slip. The lower magnitude of γ_{isf} is, the more wide the stacking fault becomes. This effect can be understood in terms of the nucleation energy barrier that the second partial of an extended dislocation would need to overcome [57]. Upon the nucleation of the leading partial (by overcoming the energy barrier γ_{us}), the second partial has to exceed
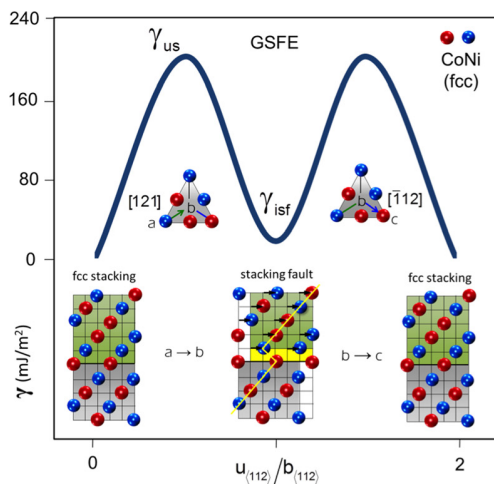
(a)
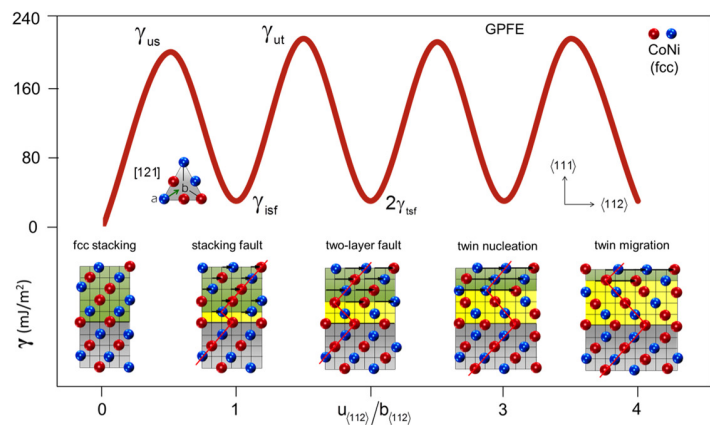
(b)
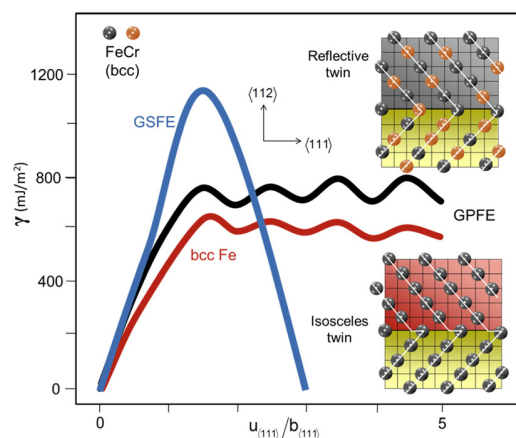
(c)

Fig. 11 (a) GSFE for Co-Ni alloys, which represents the energy pathway for the nucleation of an extended dislocation [52] connected by an intrinsic stacking fault. (b) GPFE for Co-Ni alloys [52] as an example. The GPFE represents the twinning energy pathway encompassing the formation of a single-layer intrinsic stacking fault first, then a two-layer extrinsic stacking fault, and finally a three-layer twin nucleus. Further shearing on consecutive planes results in the twin growth (migration) process. (c) Comparison among the GSFE and GPFE in bcc Fe and Fe-Cr alloys. There are two distinct types of twin boundaries in bcc alloys, namely, isosceles and reflective ones [71], which are favored differently from one material (e.g., Fe) to another (e.g., Fe-Cr).
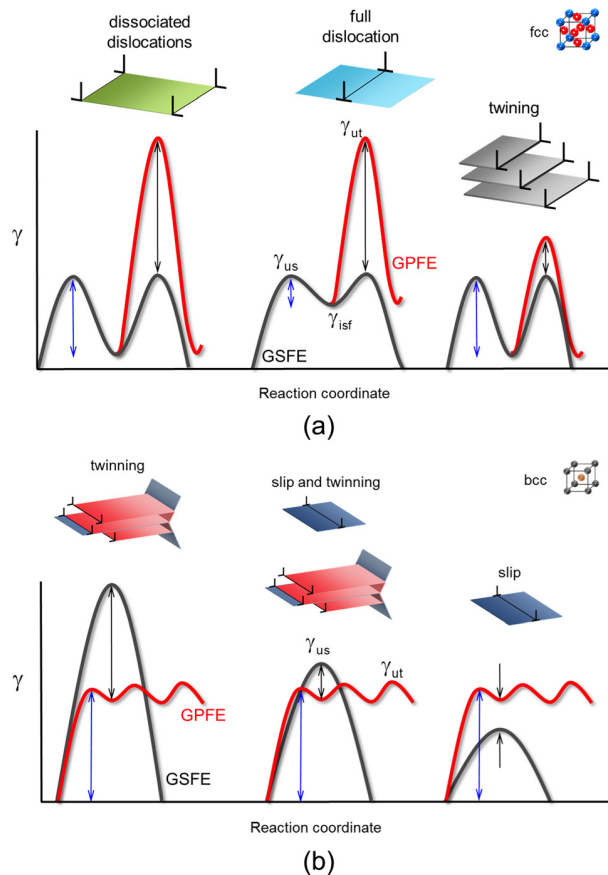
Fig. 12 (*a*) Relative sizes of the fault energetics (GSFE and GPFE) and their implication regarding the preference for a certain defect nucleation for fcc lattice [3,58–60] and (*b*) possible shapes of fault energy surfaces and the likely defect mechanism scenario in bcc lattice

a quantity equal to ($\gamma_{us} - \gamma_{isf}$). That is to say, a large difference between γ_{isf} and γ_{us} would promote splitting of full dislocations into partials. On the same rationale, in materials where both the γ_{ut} and the γ_{isf} have high magnitudes, the plasticity would be dominated by full dislocations. The effect of high γ_{ut} corresponds to the preclusion of twinning process, while the high γ_{isf} makes the creation of stacking fault difficult. In other words, lower magnitudes of both γ_{ut} and γ_{isf} levels would favor twinning.

Similar energetic rationale could also be employed for defect nucleation in bcc lattices as presented in Fig. 12(*b*). The γ_{isf} in bcc lattice is generally large, thus making the existence of a monolayer of stacking fault improbable. Therefore, we consider fault energy scenario with a high and constant γ_{isf}. With a considerably large γ_{us}, the mechanical twinning would be a preferred defect nucleation scenario. When the γ_{us} and the γ_{ut} levels are comparable, it is possible to have both slip and twinning. For the case when the γ_{us} is smaller, the material would tend to deform via slip only. Table 1 lists a compilation of DFT and experimental data on the parameters γ_{isf}, γ_{us}, and γ_{ut} (from Ref. [61]).

5 Prediction of Critical Stresses Related to Deformation Twinning

5.1 Earlier Theories on Twin Nucleation. It is now accepted that deformation twinning occurs via a succession of Shockley partials on adjacent planes. Consecutive shearing of lattice first creates an intrinsic stacking fault, then an extrinsic one (i.e., a two-layer fault), and finally a three-layer twin. After the

nucleation of the twin embryo, the subsequent gliding results in the twin migration process. These considerations are reflected in numerous twin nucleation models in the earlier literature. On phenomenological grounds, significant recent theoretical progresses are made [62,63]. Mechanistically, a number of researches earlier were geared at predicting twinning stress.

Venables [64] predicted the critical twin nucleation stress founded on the overcoming of frictional resistance to generate an intrinsic stacking fault. Afterward, Pirouz [65] considered the motions of a leading and a trailing partial dislocation bound by a stacking fault. Moreover, Miura et al. [66] introduced an extrinsic stacking fault as a condition for the nucleation of a twin embryo. Karaman et al. [50] built on these very ideas and extended to modeling solute effects on the twinning stress. Extensive Eshelby type analyses were undertaken by Meyers et al. [67]. Consequently, there were able to incorporate deformation kinetics considerations (i.e., strain rate, temperature, etc.). We note that all these theories essentially take into account the role of intrinsic stacking fault energy (γ_{isf}) as the primary material input for predicting twinning stress.

Fischer et al. [68] formulated twinning stress based on thermodynamics-based energy balance. This approach took note of the geometrical considerations such as arrangement of dislocations. The need for incorporating atomistic energetics was brought into attention by Tadmor and coworkers [59,69]. They demonstrated that material twinnability (via a case study in fcc materials) can be evaluated with the aid of fault energies, i.e., γ_{isf}, γ_{us}, and γ_{ut}. It was evident from their work that the unstable energies (γ_{us} and γ_{ut}) are equally crucial to establish a comprehensive twinning criterion along with more traditionally used γ_{isf}. Now, twin nucleation, according to these models, is triggered by the presence of a sufficiently high local stress concentration source (e.g., dislocation pile-up [64], Lomer–Cottrell barrier [50,65], grain boundary [66], dislocation wall [68], microcrack [59]). Twin nucleation propensity in the bulk of the material would indicate the inherent material propensity for such deformation mechanism. In the regard, the recent developments on the utilization of GSFE or GPFE curves are worth mentioning. For instance, Kibey et al. [70] proposed a closed-form equation for the twinning stress prediction, which utilized DFT-computed GPFE levels both in elemental metals and alloys. Thus, intricate effects of interactions between substitutional solutes and host atoms such as the so-called Suzuki segregation (discussed later) were captured.

5.2 Recent Models on Twin Nucleation. Recent models for predicting twin nucleation stress in bulk crystal configuration (i.e., in absence of any source as mentioned earlier) utilized the atomistic γ surfaces [52,71]. These approaches consider the fundamental Peierls–Nabarro-based assumptions of slip disregistry (i.e., elastic distortion caused by the presence of slip) [72–75]. Such an approach inherently permits the considerations of slip, intrinsic/extrinsic stacking fault generation prior to twin formation. The fundamental premise for predicting CRSS for twin nucleation (τ_{CRSS}^{twin}) is that the applied mechanical work ought to overcome the total energy expenditure as in the below equation:

Table 1 A summary of literature data on the γ_{isf}, γ_{us}, and γ_{ut} for various fcc metals for comparison [61]

Materials	γ_{isf} (mJm^{-2})	γ_{us} (mJm^{-2})	γ_{ut} (mJm^{-2})
Pb	49	87	92
Ag	18	133	143
Au	33	134	148
Cu	41	180	200
Ni	110	273	324
Pd	168	287	361
Pt	324	339	486
Al	130	162	215

Table 2 Comparison of theoretical and experimental twin nucleation stresses in bcc materials [71] (see text for equation details)

Materials	Major input parameters for prediction	Predicted, $\tau_{\text{CRSS}}^{\text{twin}}$ (MPa)	Experimental, $\tau_{\text{CRSS}}^{\text{twin}}$ (MPa)
Fe-3%V	$a = 0.2866$ nm $\gamma_{\text{us}} = 615$ mJm^{-2} $\gamma_{\text{ut}} = 596$ mJm^{-2}	109	90
Fe	$a = 0.2851$ nm $\gamma_{\text{us}} = 617$ mJm^{-2} $\gamma_{\text{ut}} = 628$ mJm^{-2}	190	170
Fe-50%Cr	$a = 0.2851$ nm $\gamma_{\text{us}} = 1060$ mJm^{-2} $\gamma_{\text{ut}} = 752$ mJm^{-2}	218	203 ± 13
Fe-25%Ni	$a = 0.2882$ nm $\gamma_{\text{us}} = 525$ mJm^{-2} $\gamma_{\text{ut}} = 549$ mJm^{-2}	377	398

Note: The Burgers vector (**b**) for twinning partial is $(a/6)\langle 111 \rangle$ (i.e., $b = a\sqrt{3}/6$), where a is the alloy-specific lattice constant.

$$\underbrace{td\varepsilon_{\text{twin}}\tau_{\text{CRSS}}^{\text{twin}}}_{\text{applied work}} = \underbrace{E_{\text{interaction}} + E_{\text{GPFE-nucleation}}}_{\text{energy cost}} \qquad (1)$$

where t, d, and $\varepsilon_{\text{twin}}$ are twin thickness, length, and shear strain, respectively. Typically, the relationship, $d \approx 10t$, is considered for an embryonic twin [76,77]. The elastic interaction energy ($E_{\text{interaction}}$) among twinning dislocations can be obtained from classical formulations as follows [78]:

$$E_{\text{interaction}} = \frac{\mu b_{\text{twin}}^2}{4\pi(1-v)} \left(\ln \frac{D}{d_{1-2}} + \ln \frac{D}{d_{2-3}} + \ln \frac{D}{d_{1-3}} \right) \qquad (2)$$

where D is the single crystal size; μ is the shear modulus; and d_{1-2} is the distance between dislocation "1" and "2." The spacings among the twinning dislocations are: $d_{1-3} = (\mu b_{\text{twin}}^2/2\pi\gamma_{\text{isf}})$, $d_{2-3} = 0.732 d_{1-3}$ and $d_{1-2} = d_{1-3} - d_{2-3}$ upon balancing the acting elastic forces [41]. The term $E_{\text{GPFE-nucleation}}$ represents the area underneath the GPFE curve which corresponds to the portion of twin nucleation. Equation (1) can be solved for $\tau_{\text{CRSS}}^{\text{twin}}$. Thus, predicted results on several bcc materials are compared with the experimental values (pure bcc Fe, Fe-3%V, Fe-50%Cr, and Fe-25%Ni) in Table 2 [71]. The predicted levels of $\tau_{\text{CRSS}}^{\text{twin}}$ fcc Co-Ni alloys are presented in Table 3.

For the case of a pre-existent dislocation arrangement present in the vicinity, the movement of an approaching twin nucleus would be restricted (Fig. 13). Slip–twin interaction may lead to twin migration process, which is the growth or shrinkage of a preexistent twin after the embryonic twin is nucleated [7,79]. Elastic

properties of dislocation arrays (i.e., their interaction with approaching dislocations) have been studied extensively by Li et al. [80–82]. Building on these foundations, a recent model [52] included the GPFE considerations and predicted $\tau_{\text{CRSS}}^{\text{twin-slip}}$ with accuracy. As sketched in Fig. 13, such a problem essentially involves interactions among the twinning slip ($i = 1, 2,$ and 3) and the "wall" of dislocation dipoles ($j = 1, 2, 3, \ldots, N_{\text{dipole}}$).

The consideration of dipole array is rationalized on the basis of energetic stability of the configuration as established earlier by Neumann [83]. The amount of applied work, $W_{\text{applied}} = td\varepsilon_{\text{twin}}\tau_{\text{CRSS}}^{\text{twin-slip}}$, needs to overcome the total energy expense: (i) the interaction among the wall and the twinning dislocations ($E_{\text{twin-wall interaction}}$) and (ii) the atomistic shear ($E_{\text{GPFE-migration}}$). An expression similar to Eq. (1) can be derived and solved for $\tau_{\text{CRSS}}^{\text{twin-slip}}$. The term $E_{\text{twin-wall interaction}}$ is evaluated in a similar manner as in Eq. (2). The $E_{\text{GPFE-migration}}$ represents the area underneath the GPFE curve corresponding to the migration portion. The predicted level of twin–slip interaction ($\tau_{\text{CRSS}}^{\text{twin-slip}}$) for fcc Co-Ni alloys is presented in Table 3. A comparison is made with a single slip nucleation stress ($\tau_{\text{CRSS}}^{\text{twin}}$) and ($\tau_{\text{CRSS}}^{\text{slip}}$) and the associated experimental magnitudes.

6 Annealing Twins and Associated Modeling

6.1 Nanotwinned Microstructure. Experimental reports [84,85] noted the superior strength and ductility of metallic materials rife with nanosized annealing twins (i.e., the pre-existent ones). Given the limitations of the experimental techniques to

Table 3 Comparison between the theoretical and the experimental CRSS levels for slip nucleation, twin nucleation, and twin–slip interaction in fcc Co-33%Ni alloy [52]

| Mechanism	Equations	Input parameters	Theoretical, τ_{CRSS} (MPa)	Experimental, τ_{CRSS} (MPa)
Slip nucleation	$\tau_{\text{CRSS}}^{\text{slip}} = \frac{1}{b} \left. \frac{\partial E_{\text{GSFE}}(\gamma_{\text{isf}}, \gamma_{\text{us}})}{\partial u} \right|_{\text{max}}$	$\gamma_{\text{us}} = 205$ mJ/m^2 $\gamma_{\text{isf}} = 20$ mJ/m^2 $b = a_{\text{Co-Ni}}/\sqrt{6}$ $a_{\text{Co-Ni}} = 3.521\ A^o$	14	15
Twin nucleation	$\tau_{\text{CRSS}}^{\text{twin}} = \frac{E_{\text{interaction}} + E_{\text{GPFE-nucleation}}(\gamma_{\text{tsf}}, \gamma_{\text{ut}})}{tw\varepsilon_{\text{twin}}}$	$\gamma_{\text{ut}} = 216$ mJ/m^2 $\gamma_{\text{tsf}} = 10$ mJ/m^2 $t = 3a_{\text{Co-Ni}}/\sqrt{3}$ $w \approx 10t$ $\varepsilon_{\text{twin}} = 1/\sqrt{2}$	26	27
Onset of twin-slip interaction	$\tau_{\text{CRSS}}^{\text{twin-slip}} = \frac{E_{\text{twin-wall interaction}} + E_{\text{GPFE-migration}}(\gamma_{\text{tsf}}, \gamma_{\text{ut}})}{td\varepsilon_{\text{twin}}}$	$\gamma_{\text{ut}} = 216$ mJ/m^2 $\gamma_{\text{tsf}} = 10$ mJ/m^2 $d \approx 3$ nm $\varepsilon_{\text{twin}} = 1/\sqrt{2}$	38	39
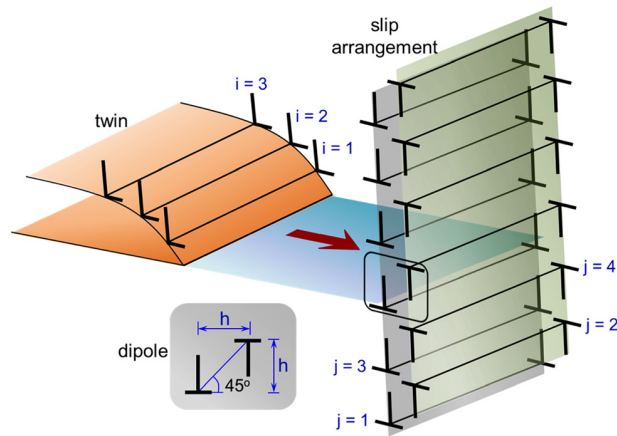
Fig. 13 Modeling of twin–slip interaction based on dislocation mechanics whereby a propagating three-layer twin approaches a dislocation dipole arrangement [52]. The atomistic contributions are considered in the form of GPFE representing the discrete lattice during the process.

capture the physical processes at the nanoscale, these findings prompted various noncontinuum modeling approaches such as molecular dynamics simulations [23,27,86]. From a mesoscale perspective, the role of annealing twins on macroscopic mechanical behavior has been also addressed on the ground of deformation kinetics principles [87,88]. The primary effect of introducing stable nanotwins in the material microstructure is found to subdivide host grains, leading to a markedly decreased activation volume (on the order of several b^3; b being the Burgers vector) for a refined microstructure [89,90]. For conventional coarse-grained material, the activation volume is typically on the order of $>1000b^3$. Intuitively, a greater degree of applied shear stress would be required to initiate and sustain plastic flow in a microstructural environment nonconductive to widespread slip. As a result, the critical resolved shear stress (hence, macroscale yield strength) would be considerably enhanced. It has been suggested that a wide variation in the slip transfer mechanisms past a coherent twin boundary plays a significant role in dictating toughness.

6.2 Slip Transfer Mechanisms past Coherent Twin Boundaries. The nature of various slip–twin boundary interception outcomes in fcc crystals has been scrutinized rigorously in the literature using experimental techniques [19,22,30,91,92], and also with theoretical treatments [26,27,93–96]. The important roles of individual mechanisms on the hardening behavior of fcc metals and alloys have been predicted elaborately. These treatments bring into attention the promise of considering different strain transfer mechanisms across the interface into a comprehensive deformation theory for nanotwinned materials. The occurrence of various slip-coherent twin boundary reactions is found to be strongly dependent on the relative Schmid factors on the twin boundary, incident, and outgoing slip systems [97]. Five most commonly observed slip transfer mechanisms past a twin boundary are: (a) incorporation, (b) transmission, (c) multiplication, (d) transmission and incorporation, and (e) blockage by a Lomer lock formation. Molecular dynamics studies of these reactions by various researchers are presented in Fig. 14 (from Refs. [23], [25], [27], [94], and [98]).

The impinging slip results in incorporation upon the boundary, provided the relative Schmid factor on the interface is very high (i.e., a situation conducive to a twin migration process) [26,27,99]. It is important to note that even though an incorporation process can be deemed as an effective blockage mechanism for oncoming slip, it does not preclude the incorporated slip continuing in a glissile motion on the twin boundary, resulting in twin growth/shrinkage [100]. On the other hand, direct transmission [22,23] occurs when the slip systems inside the twinned crystal

experience relatively high Schmid factors. Multiplication of slip [28] at the interception site transpires when the incident and the outgoing slip systems are activated with similar Schmid factors. A combination of both incorporation and transmission events [92,101,102] arises under a comparable incident/outgoing stress state, however, along with a high Schmid factor on the twin boundary. Nucleation of a Lomer lock in conjunction with a stair rod dislocation [24,25] occurs when the resolved shear stresses on incident/outgoing/boundary slip systems are all rather low. We note the fundamental difference between dislocation blockage due to incorporation (which allows continuous straining on the interface) and a Lomer lock (which precludes any glissile activity until further incidence breaks the lock). It is interesting that two of the aforementioned slip transfer mechanisms promote continuation of local straining on the interface (i.e., contribute to the twin migration process). Early literature [23] notes that the origin of considerable ductility in nanotwinned materials can be attributed to the pervasive incorporation process. We note that the most unique signature of these reaction mechanisms is the magnitude of the residual dislocation (b_r) left onto the twin boundary following the impingement.

6.3 Significance of Reaction-Specific γ_{us} and b_r at a Twin Boundary. It is intuitive that the magnitudes of the energy barrier to slip (i.e., γ_{us}) would differ to considerable extents for the individual slip transfer mechanisms. In order to compute the γ_{us} for various reactions, the "tracing atoms" method can be used in molecular dynamics simulations. As in Fig. 15, the potential energy of the tracing atoms ahead of an oncoming slip is constantly monitored. The differential between bulk and the slip-influenced potential energy, $\Delta E = E - E_{bulk}$, is computed as the slip approaches [94,103]. The insets show the position of the extended dislocation with respect to the tracing atoms, and the corresponding γ levels, which is equal to the ratio, $\Delta E / w$l after Vitek [51]. The dimensions of the tracing atomic area (w times l) are chosen judiciously to ensure convergence of the γ energy, which occurs at larger l and smaller w (Fig. 15) [104].

Using such method, Ezaz et al. [94] computed the entire GSFE curve specific to a slip–twin boundary reaction (Fig. 16) in Cu. They considered the incidence of a single dislocation upon a coherent twin boundary in the molecular dynamics simulations. It follows from their findings that the formation of Lomer lock requires overcoming the maximum energy barrier while the incorporation process has the lowest. Subsequently, Chowdhury and coworkers [52,103,105] determined the evolution of b_r as well as γ_{us} with respect to multiple slip incidence on the boundary (Fig. 10).

The saturation in the γ_{us} was attributed to the b_r achieving a steady-state magnitude with increasing incidence of slip. The origin of the saturation effect for individual case is related with precipitous rise in the local stress concentration (due to gradual accumulation of b_r) at the reaction site upon successive slip impingement. The details of b_r saturation mechanism with respect to gradual slip incidence differ from case to case; however, the fundamental mechanistic process is essentially similar. With increasing pile-up stress from the oncoming slip, the accumulated b_r eventually breaks down into multiple glissile and/or sessile slip at incidence site. With sufficiently large of approaching slip, the magnitude of b_r eventually reaches a point where a stable pattern of residual slip dissociation occurs. In the process, new glissile dislocation glide away leaving behind the b_r of the saturated magnitude. The correlations among the γ_{us}, b_r, and number of incident slip (n_{slip}) as in Fig. 10 provide invaluable energetic perspectives into the relative penetration resistances of the various strain transfer mechanisms.

References [106] and [107] modeled bcc twin–twin interaction using similar molecular dynamics simulations in Nb. Further details of the interaction mechanism between an annealing twin and a propagating one in bcc Fe-Cr lattice are investigated by Ojha et al. [71]. Under $[0\bar{1}0]$ tensile loading (far field), an
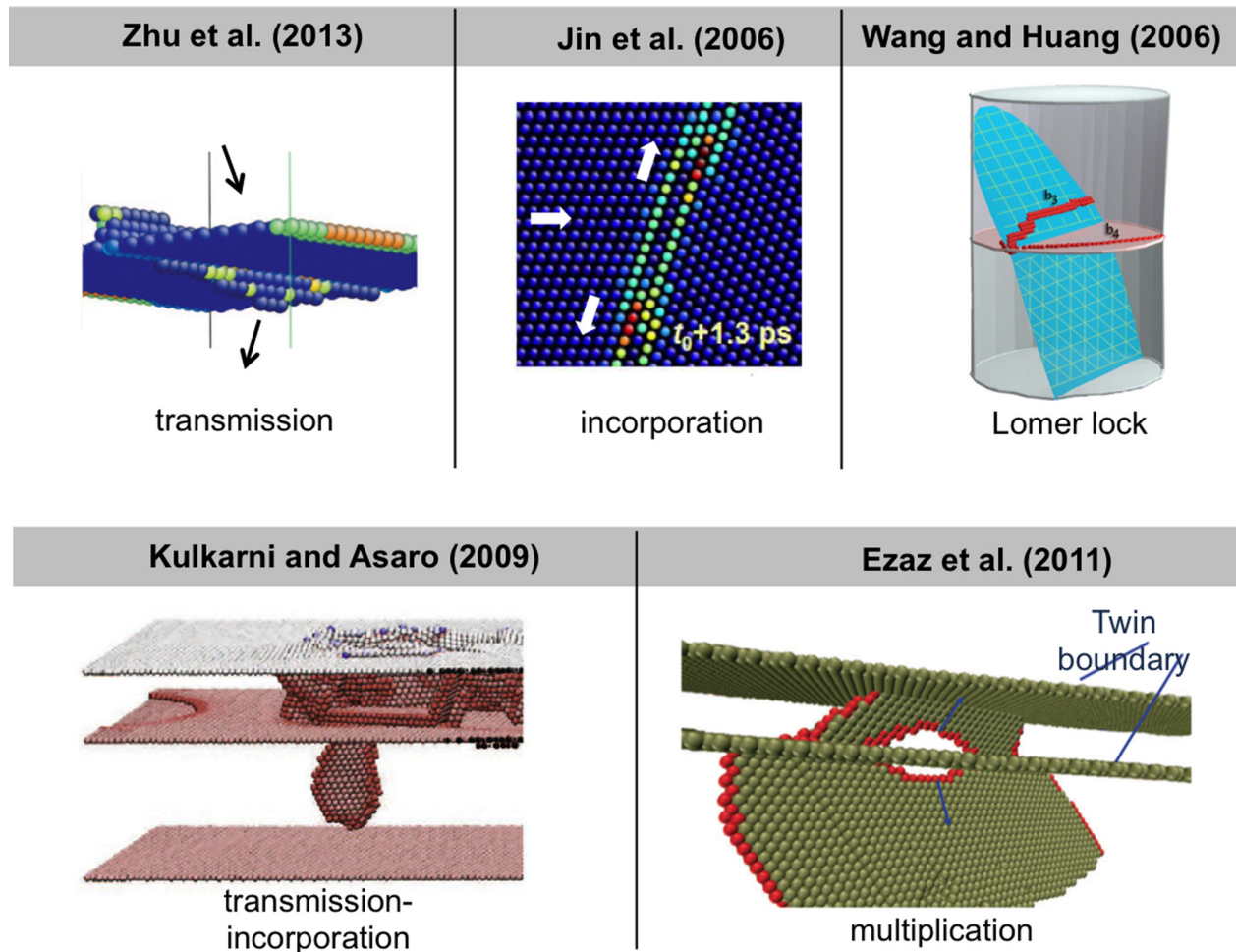
Fig. 14 Five different types of slip–twin boundary interaction mechanisms studied in molecular dynamics simulations: transmission [23], incorporation [27] (shown after 1.3 picoseconds from the beginning, t_o) Lomer lock formation [25], transmission-incorporation [98] and multiplication [94]

incoming twin consisting of three fractional dislocations of type $(a/6)\langle 111 \rangle$ impinges on the existing twin boundary as presented in Fig. 17. The ensuing process involves the incorporation of the approaching twinning partials onto the twin boundary

Fig. 15 The "tracing atom" method for computing the extrinsic magnitude of γ_{us} from molecular dynamics simulations [104]. The convergence criteria of the energy parameter are obtained at high l and low w, which are the length and width of the tracing area, respectively.

leaving a residual dislocation with Burgers vector, $\mathbf{b}_r$ (of magnitude equal to 1.0a). A compressive load along the [111] crystallographic direction results in a similar incorporate process, however, with a different b_r (equal to 0.82a). The apparent different outcomes for tension and compression cases can be attributed to the differences in the levels of Schmid factors on the activated systems.
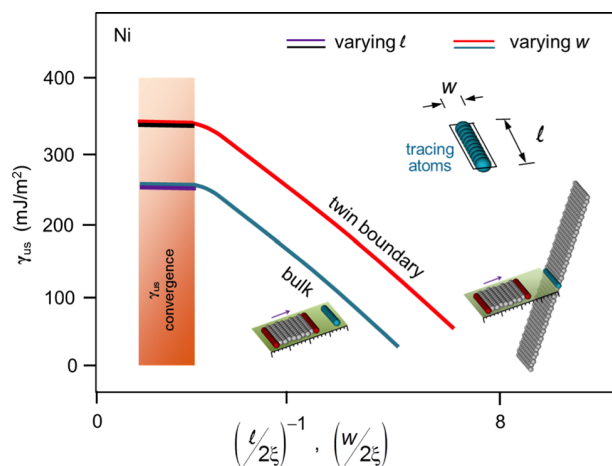
6.4 Predicting Friction Stresses for Twin-Slip or Twin–Twin Reactions. The frictional stress specific to any reaction outcome of slip intercepting a twin ($\tau_{CRSS}^{reaction}$) in the presence of $\mathbf{b}_r$ can be predicted by considering two distinct forms of energy contributions: (a) the extrinsic level of fault energy subjected to local stresses, $E_{GSFE/GPFE}$ (note that GPFE is applicable for incorporation process only) and (b) the residual elastic energy due to $\mathbf{b}_r$, $E_{residual} = E_{residual}(b_r)$ [33]. The applied stress $\tau_{CRSS}^{reaction}$ required to move an oncoming dislocation toward the boundary by a distance of ∂d is derived based on the work–energy balance as follows:

$$\underbrace{b_{incident}\tau_{CRSS}^{reaction}\partial d}_{\text{work done}} = \underbrace{\partial E_{GSFE/GPFE}(f_{disregistry}, \gamma) + \partial E(b_r)}_{\text{energy expense}} \quad (3)$$

The predicted stresses using Eq. (3) in fcc Ni-Co alloy are presented in Table 4 (also Fig. 10). Similarly, in bcc materials, the $\tau_{CRSS}^{twin-twin}$ is predicted and compared with experimental values based on single-crystal studies as in Fig. 18 [71].
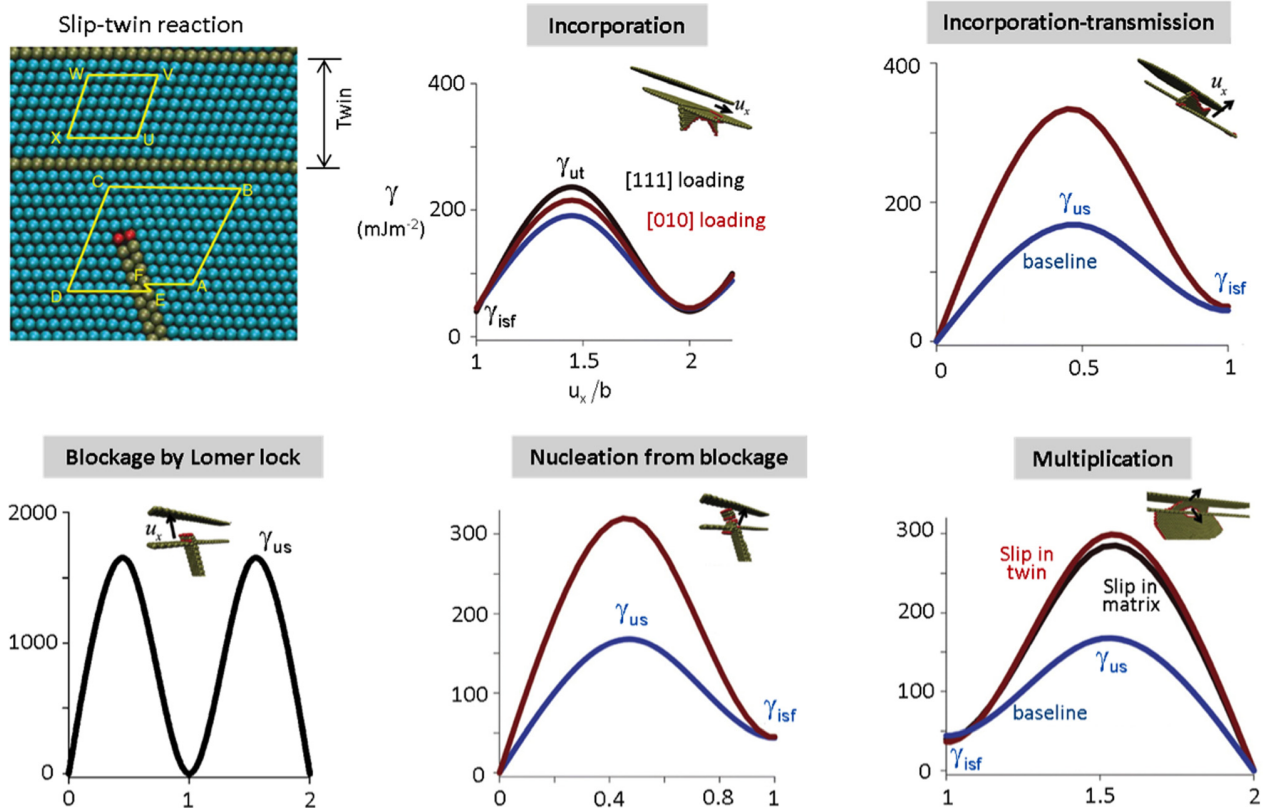
Fig. 16 Fault energy profile for various slip-coherent twin boundary interaction mechanism in fcc Cu [94]. Incorporation process has the lowest energy barrier while the blockage case has the highest. The curves designated "baseline" represents the GSFE profile for bulk lattice shearing (i.e., absence of residual slip b_r). The reason the GSFE curves specific to the reactions are elevated is that b_r creates local stress, which makes glide difficult for subsequent incidence.

To predict the $\tau_{\text{CRSS}}^{\text{poly}}$ for the polycrystalline nanotwinned Ni-Co alloys, three major flow contributions are considered: (a) the free glide stress $\tau_{\text{free glide}}$, (b) slip–twin boundary interaction stress, $\tau_{\text{CRSS}}^{\text{reaction}}$, and (c) the forest hardening stress (at a predeformation dislocation density) $\tau_{\text{forest}} = \alpha \mu b \sqrt{\rho}$ [108,109]; where α is a material constant (from 0.5 to 1) and ρ the forest dislocation density (assumed to be $10^{14}/\text{m}^2$ which is the typical predeformation literature value). The $\tau_{\text{CRSS}}^{\text{reaction}}$ is observed to be the most dominating. Using Eq. (4), we calculate the $\tau_{\text{CRSS}}^{\text{poly}}$ levels for different Ni-Co alloys based on iso-strain type mixing formulations

$$\tau_{\text{CRSS}}^{\text{poly}} = (1 - V_f)\tau_{\text{free glide}} + \sum_{\text{reaction}} V_f^{\text{reaction}} \tau_{\text{slip-twin}}^{\text{reaction}} + (1 - V_f)\tau_{\text{forest}} \quad (4)$$

where V_f is the total volume fraction of the material region hosting the aggregate slip–twin reactions; V_f^{reaction} is the assigned volume fraction for a specific reaction, i.e., $V_f = \sum_{\text{reaction}} V_f^{\text{reaction}}$. The predicted CRSS for polycrystalline Ni-Co alloys is compared in Fig. 19 with experimental ones (determined by using Taylor factor normalization for the uniaxial stress–strain data in Fig. 2(c)).
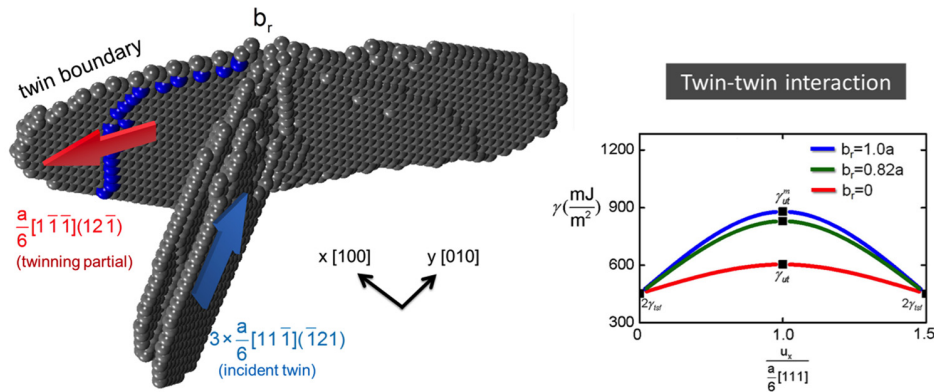

Fig. 17 An approaching twin consisting of three (a/6)[11$\bar{1}$] type twinning partials intercept a pre-existent twin boundary [71] in bcc Fe-Cr alloy. The resultant reaction is the incorporation of the twinning partials on the boundary leaving a residual dislocation (b_r) behind at the interception site. Depending on the magnitude of b_r (which can be obtained by modulating the Schmid factor or changing single crystal loading direction), the GSFE profile will be altered as shown on the right.

Twin boundary-slip interaction mechanisms	Dislocation type	b_r/a (saturated after multiple incidence)	$\tau_{CRSS}^{twin-slip}$ (MPa)
Incorporation	Screw	0.55	175
Transmission	Edge	0.76	230
Multiplication	Mixed	1.02	280
Transmission-incorporation	Mixed	1.27	336
Blockage by Lomer lock	Mixed	1.70	445

7 Further Problems: Polycrystalline Deformation, Fracture Behavior, Phase Transformation, Hexagonal Close Packed Deformation

The foregoing models have examined the single-crystal behavior without the presence of multiple grains. It is important to characterize single crystals to understand polycrystalline deformation, in that they provide insight into inherent defect evolution circumventing the effects of texture and interfaces. The plastic stress–strain behaviors of single crystals consist of three mechanistically distinct hardening regimes such as stage I, II, and III [110–112]. The initial plasticity (stage I) is dominated by massive defect nucleation (e.g., slip or twin) followed by the ensuing hardening stages characterized by more complex defect interplays. For example, the fluctuating nature of the flow is more pronounced in bcc than in fcc [30]. This could be attributed to the considerable difference in the energy barriers between twin nucleation and migration in bcc than fcc materials. These trends may be subjected to significant modifications due to the presence of material interfaces. In a multigrain environment, the presence of grain boundaries would considerably affect the overall material behaviors. The role of interfaces as obstacles to flow and/or sources of defect nucleation would give rise to different macroscale constitutive responses. For example, upon studying polycrystalline Co-33%Ni with low stacking fault energy, Remy [8] attributed the increased hardening response to the slip obstruction due to an abundance of newly generated twin boundaries. It was argued that extensive twinning subdivides a particular grain in multiple segments restricting the slip mobility, therefore, giving rise to Hall–Petch type strengthening effects. In general, conventional fcc single crystals shows twinning behavior only at very high stress [113,114] and strain rate. From a continuum standpoint, Meyers et al. [67] utilized Eshelby type analysis to theorize the strain rate, temperature effects on twinning. Similarly, in molecular dynamics-based simulations with high strain rate, many researchers investigated the mechanistic aspect of deformation in nanocrystalline multigrain configurations.

Yamakov et al. [115] considered the deformation behaviors of Al multigrained structure (Fig. 20) with an average grain diameter of 70 nm. Deformation twins are found to form at the grain boundaries. The mechanism is initiated in the form of a single partial dislocation nucleation followed by parallel and adjacent slip. Consecutive gliding of Shockley partials eventually results in a deformation twin. Similarly, Shabib and Miller uncovered the nucleation of extended stacking fault generation aided by gliding of Shockley partial dislocation, which originated at a grain boundary [116]. In an different approach, Li et al. and Zhu and Gao [117,118] studied Cu polycrystalline structures with inherent annealing twins of nanometer size. Two distinct mechanistic trends were observed as a function of twin spacing. For thinner twins (of 1.62 nm), slip nucleated parallel to the twin boundaries with no significant hardening contribution from the presence of twins. On the other hand, when the twin spacing was about 6 nm slip crisscrossed the grain and intercepted the twin boundaries giving rise to significant hardening. Upon sufficient deformation, massive slip nucleation occurs from the grain boundaries, which intercept the twins. These studies have provided important mechanistic understanding of twinning-based deformation in nanocrystalline microstructure. Energetic representation of polycrystalline deformation poses, as we envision, a promising future endeavor, which would further reveal the relative strengths of, say, various interface types, defect interaction, etc., for polycrystal deformation.

Another interesting and important application of the atomistic aspects of plasticity lies in understanding crack propagation behavior, which is a significant engineering concern in a wide range of materials [6,105,119,120]. Damage response under static or cyclic loading is decided by the irreversible plastic phenomena at the crack tip in the form of slip or twinning. Earlier Rice and coworkers [121,122] established the importance of atomistic description of crack-tip behavior. In particular, their analysis highlighted the use of the unstable stacking fault energy γ_{us} in the context of modeling cracking behavior. Subsequently, Tadmor and coworkers [59,69] conceptualized the twinnability in front of a propagating crack considering a comprehensive treatment of fault
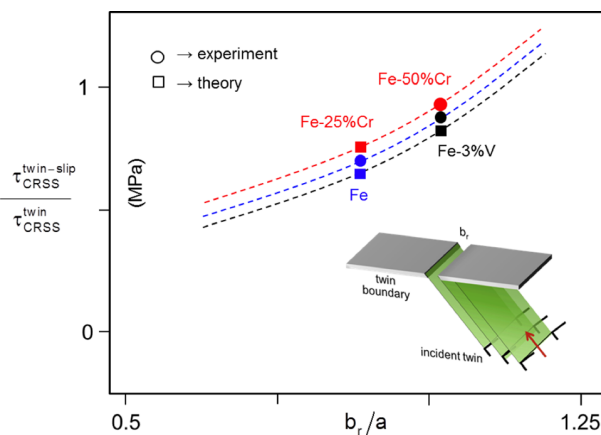

Fig. 18 Comparison between the predicted twin–twin interaction stress ($\tau_{CRSS}^{twin-twin}$) and the experimental one in several bcc alloys [71]
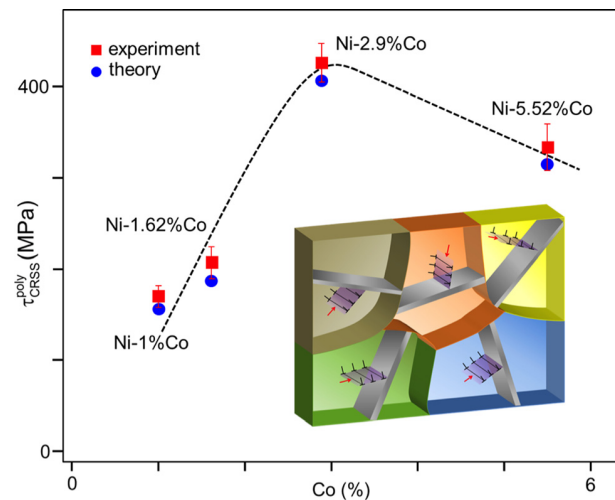

Fig. 19 Comparison between the predicted and experimental critical resolved shear stresses in polycrystalline NiCo alloys (in the presence of annealing twins) [52]
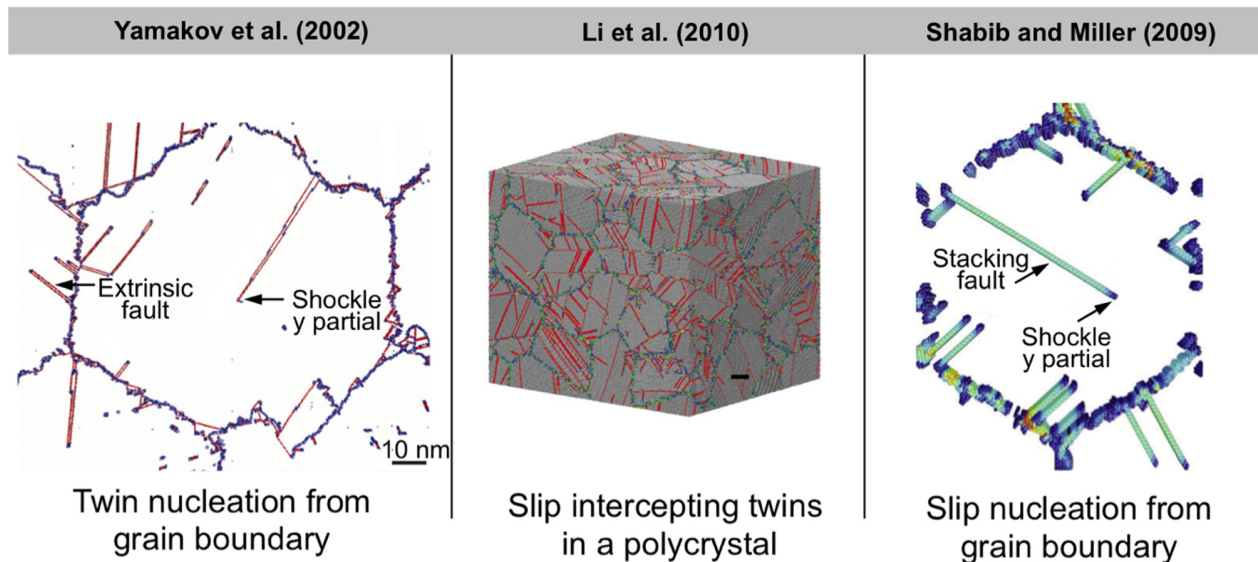
Fig. 20 Molecular dynamics simulation of polycrystalline deformation behaviors. From left to right: Nucleation of twins from grain boundaries in nanocrystalline Al [115]; a nanocrystalline Cu structure with annealing twins, which upon deformation results in massive slip–interface interactions [117]; Shockley partials emerging from grain boundaries in Cu [116].

energy parameters (i.e., γ_{isf}, γ_{us} and γ_{ut}) as in Fig. 21. They demonstrated that density functional theory-based fault energy parameters can be used to predict twinning propensity for mesoscale crack propagation. This is a significant advancement in the modeling of crack behaviors, in that they pave the way for further advancing crack modeling using atomistically computed γ surface. On molecular dynamics frontier, there have been significant progresses on fracture behaviors as well. One of the earlier studies of twinning-mediated crack propagation using molecular dynamics simulations was undertaken by deCelis et al. [123]. In their work, the critical stress intensity factor was established on the basis of atomistically sharp crack advancing via twinning in copper (Fig. 21). More recently, using molecular dynamics modeling, Warner et al. [60] study the completion of twinning with slip at a crack tip. They proposed that the relative size/shape of GSFE/GPFE curves would strongly dictate one plastic mechanism (e.g., twinning) over another (e.g., slip). Founded on these works, recent modeling efforts [124,125] have noted the incorporation of the atomistically predicted slip glide strengths into a formalism to predict cyclic damage metrics. Similarly, the friction stresses for twinning mechanism also hold considerable promise for theorizing the crack advancement problem. For materials which predominantly deform via twinning (e.g., hcp metals and alloys), such modeling can shed new light in terms of physical mechanism(s) of

cracking [126]. For the readers' benefit, a summary of relevant works discussed in the paper is provided in Table 5.

Atomistic modeling can also benefit the area of phase transformation materials such as the shape memory alloys behaviors [127–131]. For instance, the shape memory alloys (e.g., NiTi) undergo martensitic phase transformation, which is also accompanied by deformation twinning. In the last decade, a number of molecular dynamics based studies have emerged depicting the twinning phenomena [132–134] in shape recovering alloys. A comprehensive GSFE- or GPFE-based analysis could be particularly useful to understand materials deformation predilection such as competition among slip, twining, and transformation phenomena [135]. Similarly, metallic materials with hcp lattice undergo twinning dominated plasticity [136,137], which can benefit from atomistic energetics modeling [138].

8 Appropriate Use of Atomistics and Modeling Larger-Scale Deformation

One ought to account for the uncertainty of the calculations while employing atomistic quantities to derive continuum models. Applicable to both molecular dynamics and DFT-based energy calculations is the sensitivity of: (i) the method adopted for atomic relaxation and (ii) simulation supercell size. Atomic positions can
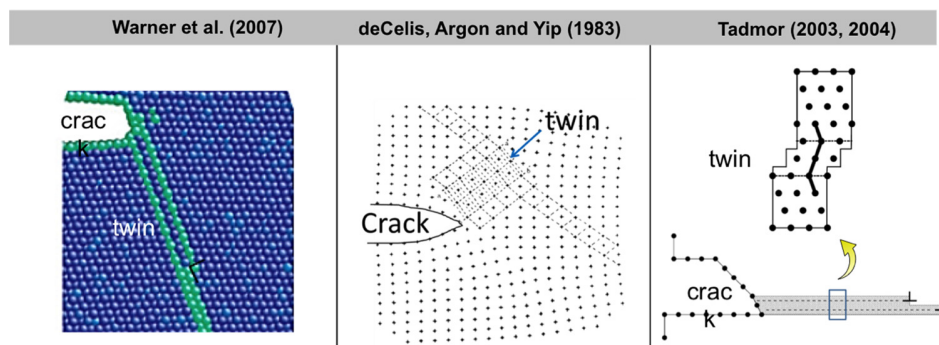

Fig. 21 Study of crack-tip twinning behavior using atomistics concept. Competition between twin and slip nucleation from a crack is correlated with the relative size/shape of GSFE/GPFE curves [59,60,69,123].

Journal of Engineering Materials and Technology   APRIL 2018, Vol. 140 / 020801-15

Table 5 Summary of theories reviewed in this paper contributing to twining energetics and critical stress prediction in fcc and bcc materials

	Investigators	Model description	Model impact
Continuum	Meyers et al. [67]	Formulating deformation kinetics of twinning	Lays foundation for continuum-based analysis of temperature and strain-rate effects of deformation twinning
	Kalidindi [62], Staroselsky and Anand [63], Fischer et al. [68]	Thermodynamic analysis of deformation twinning	Establishes a work-energy balance for twin embryo formation based on continuum dislocation mechanics
	Miura et al. [66], Karaman et al. [50]	Rationalization of twining propensity originating from alloying	Utilize γ_{isf} to predict critical stress for twin nucleation
Mesoscale	Sleeswyk [41,46], Ogawa [42], Priestner and Leslie [43], Lagerlöf [40]	Mechanism of twin embryo nucleation in bcc materials	Provides a mechanistic interpretation of twin nucleation considering dissociation of a three-fold slip core
	Cottrell and Bilby [36]	Mechanism of twin nucleus formation in bcc lattice	Explains twin nucleation with the aid of a slip acting as a source (pole) of stacking fault emission
	Venables [44,45,64]	Nucleation of twin embryo in fcc lattice via double-pole mechanism	Proposes a double pole to account for the relative ease of layer-by-layer stacking fault piling leading to twin embryo
	Remy [7,8,19]	Geometry of twinning dislocations intercepting another twin	Provides detailed analysis of Burgers vector conservation in twin–twin interactions in postyield behavior
	Mahajan and Chin [47]	Mechanism of twin nucleus formation in fcc lattice	Explains fcc twinning mechanism which occurs via interaction between two extrinsic stacking faults
Atomistics	Ogata et al. [3,4], Van Swygenhoven et al. [57], Siegel [56], Cai et al. [58]	Prediction of twinning γ energies (i.e., GPFE)	Demonstrates feasibility of utilizing modern atomistic simulations tools to compute twinning energy barriers (by rigid shear of crystal half-spaces)
	Yamakov et al. [115] Asaro and Suresh [87], Jin et al. [5,27], Zhu et al. [23], Deng and Sansoz [86], Kulkarni and Asaro [98], Shabib and Miller [116], Li et al. [117], Ezaz et al. [94]	Annealing twins (with coherent twin boundaries) influencing deformation mechanism at nanoscale	Investigates roles of pre-existent annealing twins on mechanical response
			Explores slip-coherent twin boundary interactions, their energetics, and eventual role of controlling strength and ductility
	deCelis et al. [123], Tadmor and Bernstein [59], Warner et al. [60]	Atomistics of twining as relates to crack-tip plasticity	Introduces a detailed model using energy barriers (γ_{us}, γ_{ut}) in addressing fracture problem in fcc materials
	Kibey et al. [39,76], Chowdhury et al. [52], Ojha et al. [71]	Atomistics of twinning and twin-slip interaction and prediction of critical stress	Predicts GPFE profiles for twinning in pristine lattice and also subjected to residual slip accumulation
			Predicts critical stresses for intrinsic or extrinsic twinning mechanisms

be allowed to adjust all x, y, and z coordinates (full relaxation) or the adjustments can occur only in the direction vertical to the fault plane (partial relaxation). It is important to note that the empirical potential-based fault energies can be particularly sensitive to the choice of relaxation scheme [139,140]. One reasonable method of validating empirical potential obtained calculations would be to compare them density functional theory calculations, which are considerably less susceptible to such artifacts. One should also be careful regarding the simulation supercell size as well as the boundary conditions. For instance, the number of layers in the direction vertical to the glide plane considered during the rigid shear simulations needs to large enough to reach energetic convergence. To simulate bulk properties in molecular dynamics, the system size ought to be sufficiently large such that physical observables (i.e., the total energy, entropy) converge regardless of further increase in the supercell volume. This can be established by conducting multiple simulations with varying dimensions (x, y, and z) of representative volume element. Once the correct level of convergence of atomistic parameters is ascertained, their incorporation into the prediction of continuum-scale CRSS levels would lead to better agreement with the experimental values. Another concern of importance is the introduction of nonsystematic error in DFT calculations. For example, the small errors in lattice constant

of the defect plane can move since the interplanar spacing is a function of lattice constant, a small error in the lattice constant magnitude can lead to over- or under-estimation of atomic distances. One possible way to eliminate accumulation of such errors is the usage of average experimental lattice constant in establishing the large deformation cell while permitting local relaxations [141].

From modeling standpoint, the CRSS levels represent the initial stage of plasticity, i.e., immediately following the elastic deformation. The macroscopic yielding of materials is primarily decided by overcoming the critical resolved shear stresses at the microscale. Hence, it is reasonable and sufficient to consider only the lattice friction resistance. Evidently, the scope of such approach does not yet address the entire spectrum of the material stress–strain behavior particularly the aspect of massive defect evolution. The current length scales associated with atomistic modeling are confined to nanometers. However, the postyield deformation mechanics would be primarily governed by extensive defect interactions, the exact nature of which nature will decide the macroscopic flow behavior. The strengthening attributes during the dynamic evolution of defects are large decided by the complex assortment of plastic mechanisms. As promising future refinement in modeling efforts, the development of a combined atomistic and mesoscopic modeling platform would serve such a

need. For instance, the discrete lattice effects need to be bridged via extensive mesoscale defect modeling (e.g., dislocation dynamics) [142–144] and/or deformation kinetics [145]. It should be noted that the models address within atomistic framework do not incorporate the role of thermal and rate-dependent phenomena. In order to address the temperature and strain-rate effects, the atomistic theory could be modified with the principles of the deformation kinetics [145,146]. The plastic flow mechanisms that are dependent on the deformation rate/temperature abide by the Arrhenius laws, which dictate an exponential dependence on an energy barrier to be overcome. In that regard, the current calculations consider the efficacy of the unstable stacking fault energy, γ_{us}, being the most deciding energy barrier parameter to quantify the resistance to plastic flow.

Funding Data

References

[1] Tucker, G. J., and Foiles, S. M., 2015, "Quantifying the Influence of Twin Boundaries on the Deformation of Nanocrystalline Copper Using Atomistic Simulations," Int. J. Plast., 65, pp. 191–205.

[2] Li, J., Ngan, A. H., and Gumbsch, P., 2003, "Atomistic Modeling of Mechanical Behavior," Acta Mater., 51(19), pp. 5711–5742.

[3] Ogata, S., Li, J., and Yip, S., 2005, "Energy Landscape of Deformation Twinning in Bcc and Fcc Metals," Phys. Rev. B, 71(22), p. 224102.

[4] Ogata, S., Li, J., and Yip, S., 2002, "Ideal Pure Shear Strength of Aluminum and Copper," Science, 298(5594), pp. 807–811.

[5] Jin, Z. H., Dunham, S. T., Gleiter, H., Hahn, H., and Gumbsch, P., 2011, "A Universal Scaling of Planar Fault Energy Barriers in Face-Centered Cubic Metals," Scr. Mater., 64(7), pp. 605–608.

[6] Chowdhury, P., and Sehitoglu, H., 2016, "Mechanisms of Fatigue Crack Growth—A Critical Digest of Theoretical Developments," Fatigue Fract. Eng. Mater. Struct., 39(6), pp. 652–674.

[7] Remy, L., 1977, "Twin-Twin Interaction in FCC Crystals," Scr. Metall., 11(3), pp. 169–172.

[8] Remy, L., 1978, "Kinetics of Fcc Deformation Twinning and Its Relationship to Stress-Strain Behaviour," Acta Metall., 26(3), pp. 443–451.

[9] McPhie, M., Berbenni, S., and Cherkaoui, M., 2012, "Activation Energy for Nucleation of Partial Dislocation From Grain Boundaries," Comput. Mater. Sci., 62, pp. 169–174.

[10] Warner, D. H., Sansoz, F., and Molinari, J. F., 2006, "Atomistic Based Continuum Investigation of Plastic Deformation in Nanocrystalline Copper," Int. J. Plast., 22(4), pp. 754–774.

[11] M'Guil, S., Wen, W., Ahzi, S., Gracio, J. J., and Davies, R. W., 2015, "Analysis of Shear Deformation by Slip and Twinning in Low and High/Medium Stacking Fault Energy Fcc Metals Using the ϕ-Model," Int. J. Plast., 68, pp. 132–149.

[12] Sun, C. Y., Guo, N., Fu, M. W., and Wang, S. W., 2016, "Modeling of Slip, Twinning and Transformation Induced Plastic Deformation for TWIP Steel Based on Crystal Plasticity," Int. J. Plast., 76, pp. 186–212.

[13] Müllner, P., and Romanov, A., 2000, "Internal Twinning in Deformation Twinning," Acta Mater., 48(9), pp. 2323–2337.

[14] Tadmor, E. B., and Miller, R. E., 2011, Modeling Materials: Continuum, Atomistic and Multiscale Techniques, Cambridge University Press, Cambridge, UK.

[15] Jo, M., Koo, Y. M., Lee, B.-J., Johansson, B., Vitos, L., and Kwon, S. K., 2014, "Theory for Plasticity of Face-Centered Cubic Metals," Proc. Natl. Acad. Sci., 111(18), pp. 6560–6565.

[16] Li, W., Lu, S., Hu, Q.-M., Kwon, S. K., Johansson, B., and Vitos, L., 2014, "Generalized Stacking Fault Energies of Alloys," J. Phys.: Condens. Matter, 26(26), p. 265005.

[17] Lebensohn, R., and Tomé, C., 1993, "A Self-Consistent Anisotropic Approach for the Simulation of Plastic Deformation and Texture Development of Polycrystals: Application to Zirconium Alloys," Acta Metall. Mater., 41(9), pp. 2611–2624.

[18] Chowdhury, P. B., 2016, "Modeling Mechanical Properties–Linking Atomistics to Continuum," Ph.D. thesis, University of Illinois at Urbana-Champaign, Urbana, IL.

[19] Remy, L., 1981, "The Interaction Between Slip and Twinning Systems and the Influence of Twinning on the Mechanical Behavior of Fcc Metals and Alloys," Metall. Trans. A, 12(3), pp. 387–408.

[20] Wang, J., Anderoglu, O., Hirth, J. P., Misra, A., and Zhang, X., 2009, "Dislocation Structures of $\Sigma 3$ {112} Twin Boundaries in Face Centered Cubic Metals," Appl. Phys. Lett., 95(2), p. 021908.

[21] Sutton, A. P., and Balluffi, R. W., 1995, "Interfaces in Crystalline Materials," Phys. Today, 49(9), p. 88.

[22] Kacher, J., Eftink, B., Cui, B., and Robertson, I., 2014, "Dislocation Interactions With Grain Boundaries," Curr. Opin. Solid State Mater. Sci., 18(4), pp. 227–243.

[23] Zhu, T., Li, J., Samanta, A., Kim, H. G., and Suresh, S., 2007, "Interfacial Plasticity Governs Strain Rate Sensitivity and Ductility in Nanostructured Metals," Proc. Natl. Acad. Sci., 104(9), pp. 3031–3036.

[24] Karnthaler, H., 1978, "The Study of Glide on {001} Planes in Fcc Metals Deformed at Room Temperature," Philos. Mag. A, 38(2), pp. 141–156.

[25] Wang, J., and Huang, H., 2006, "Novel Deformation Mechanism of Twinned Nanowires," Appl. Phys. Lett., 88(20), p. 203112.

[26] Asaro, R. J., and Kulkarni, Y., 2008, "Are Rate Sensitivity and Strength Effected by Cross-Slip in Nano-Twinned Fcc Metals," Scr. Mater., 58(5), pp. 389–392.

[27] Jin, Z.-H., Gumbsch, P., Ma, E., Albe, K., Lu, K., Hahn, H., and Gleiter, H., 2006, "The Interaction Mechanism of Screw Dislocations With Coherent Twin Boundaries in Different Face-Centered Cubic Metals," Scr. Mater., 54(6), pp. 1163–1168.

[28] Miller, B., Fenske, J., Su, D., Li, C.-M., Dougherty, L., and Robertson, I. M., 2006, "Grain Boundary Responses to Local and Applied Stress: An In Situ TEM Deformation Study," Symposium EE at the MRS Fall Meeting, Boston, MA, Nov. 27–Dec. 1, Paper No. 0976-EE02-01.

[29] Frenkel, D., and Smit, B., 2001, Understanding Molecular Simulation: From Algorithms to Applications, Academic Press, Cornwell, UK.

[30] Christian, J. W., and Mahajan, S., 1995, "Deformation Twinning," Prog. Mater. Sci., 39(1), pp. 1–157.

[31] Beyerlein, I. J., Zhang, X., and Misra, A., 2014, "Growth Twins and Deformation Twins in Metals," Annu. Rev. Mater. Res., 44, pp. 329–363.

[32] Zhu, Y. T., Liao, X., and Wu, X., 2012, "Deformation Twinning in Nanocrystalline Materials," Prog. Mater. Sci., 57(1), pp. 1–62.

[33] Chowdhury, P., Sehitoglu, H., Maier, H., and Rateick, R., 2015, "Strength Prediction in NiCo Alloys—The Role of Composition and Nanotwins," Int. J. Plast., 79, pp. 237–258.

[34] Patriarca, L., Abuzaid, W., Sehitoglu, H., Maier, H. J., and Chumlyakov, Y., 2013, "Twin Nucleation and Migration in FeCr Single Crystals," Mater. Charact., 75, pp. 165–175.

[35] Patriarca, L., Abuzaid, W., Sehitoglu, H., and Maier, H. J., 2013, "Slip Transmission in Bcc FeCr Polycrystal," Mater. Sci. Eng. A, 588, pp. 308–317.

[36] Cottrell, A., and Bilby, B., 1951, "LX. A Mechanism for the Growth of Deformation Twins in Crystals," London, Edinburgh, Dublin Philos. Mag. J. Sci., 42(329), pp. 573–581.

[37] Li, S., Ding, X., Deng, J., Lookman, T., Li, J., Ren, X., Sun, J., and Saxena, A., 2010, "Superelasticity in Bcc Nanowires by a Reversible Twinning Mechanism," Phys. Rev. B, 82(20), p. 205435.

[38] Harding, J., 1967, "The Yield and Fracture Behaviour of High-Purity Iron Single Crystals at High Rates Crystals of Strain," Proc. R. Soc. London A, 299(1459), pp. 464–490.

[39] Kibey, S., Liu, J., Johnson, D., and Sehitoglu, H., 2007, "Energy Pathways and Directionality in Deformation Twinning," Appl. Phys. Lett., 91(18), p. 181916.

[40] Lagerlöf, K., 1993, "On Deformation Twinning in Bcc Metals," Acta Metall. Mater., 41(7), pp. 2143–2151.

[41] Sleeswyk, A., 1963, "$^{1}/_{2}$<111> Screw Dislocations and the Nucleation of {112}<111> Twins in the Bcc Lattice," Philos. Mag., 8(93), pp. 1467–1486.

[42] Ogawa, K., 1965, "Edge Dislocations Dissociated in {112} Planes and Twinning Mechanism of Bcc Metals," Philos. Mag., 11(110), pp. 217–233.

[43] Priestner, R., and Leslie, W., 1965, "Nucleation of Deformation Twins at Slip Plane Intersections in BCC Metals," Philos. Mag., 11(113), pp. 895–916.

[44] Venables, J., 1961, "Deformation Twinning in Face-Centred Cubic Metals," Philos. Mag., 6(63), pp. 379–396.

[45] Venables, J., 1974, "On Dislocation Pole Models for Twinning," Philos. Mag., 30(5), pp. 1165–1169.

[46] Sleeswyk, A., 1974, "Perfect Dislocation Pole Models for Twinning in the Fcc and Bcc Lattices," Philos. Mag., 29(2), pp. 407–421.

[47] Mahajan, S., and Chin, G., 1973, "Formation of Deformation Twins in Fcc Crystals," Acta Metall., 21(10), pp. 1353–1363.

[48] Blewitt, T., Coltman, R., and Redman, J., 1957, "Low-Temperature Deformation of Copper Single Crystals," J. Appl. Phys., 28(6), pp. 651–660.

[49] Jin, Z., and Bieler, T. R., 1995, "An In-Situ Observation of Mechanical Twin Nucleation and Propagation in TiAl," Philos. Mag. A, 71(5), pp. 925–947.

[50] Karaman, I., Sehitoglu, H., Gall, K., Chumlyakov, Y., and Maier, H., 2000, "Deformation of Single Crystal Hadfield Steel by Twinning and Slip," Acta Mater., 48(6), pp. 1345–1359.

[51] Vitek, V., 1968, "Intrinsic Stacking Faults in Body-Centred Cubic Crystals," Philos. Mag., 18(154), pp. 773–786.

[52] Chowdhury, P., Sehitoglu, H., Abuzaid, W., and Maier, H., 2015, "Mechanical Response of Low Stacking Fault Energy Co–Ni Alloys—Continuum, Mesoscopic and Atomic Level Treatments," Int. J. Plast., 71, pp. 32–61.

[53] Chandran, M., and Sondhi, S., 2011, "First-Principle Calculation of Stacking Fault Energies in Ni and Ni-Co Alloy," J. Appl. Phys., 109(10), p. 103525.

[54] Zhou, X., Johnson, R., and Wadley, H., 2004, "Misfit-Energy-Increasing Dislocations in Vapor-Deposited CoFe/NiFe Multilayers," Phys. Rev. B, 69(14), p. 144113.

[55] Pun, G. P., and Mishin, Y., 2012, "Embedded-Atom Potential for Hcp and Fcc Cobalt," Phys. Rev. B, 86(13), p. 134116.

[56] Siegel, D. J., 2005, "Generalized Stacking Fault Energies, Ductilities, and Twinnabilities of Ni and Selected Ni Alloys," Appl. Phys. Lett., 87(12), p. 121901.

[57] Van Swygenhoven, H., Derlet, P., and Frøseth, A., 2004, "Stacking Fault Energies and Slip in Nanocrystalline Metals," Nat. Mater., 3(6), pp. 399–403.

[58] Cai, T., Zhang, Z. J., Zhang, P., Yang, J. B., and Zhang, Z. F., 2014, "Competition Between Slip and Twinning in Face-Centered Cubic Metals," J. Appl. Phys., 116(16), p. 163512.

[59] Tadmor, E., and Bernstein, N., 2004, "A First-Principles Measure for the Twinnability of FCC Metals," J. Mech. Phys. Solids, **52**(11), pp. 2507–2519.

[60] Warner, D. H., Curtin, W. A., and Qu, S., 2007, "Rate Dependence of Crack-Tip Processes Predicts Twinning Trends in Fcc Metals," Nat. Mater., **6**(11), pp. 876–881.

[61] Kibey, S. A., 2007, "Mesoscale Models for Stacking Faults, Deformation Twins and Martensitic Transformations: Linking Atomistics to Continuum," Ph.D. thesis, University of Illinois at Urbana-Champaign, Urbana, IL.

[62] Kalidindi, S. R., 1998, "Incorporation of Deformation Twinning in Crystal Plasticity Models," J. Mech. Phys. Solids, **46**(2), pp. 267–290.

[63] Staroselsky, A., and Anand, L., 1998, "Inelastic Deformation of Polycrystalline Face Centered Cubic Materials by Slip and Twinning," J. Mech. Phys. Solids, **46**(4), pp. 671–696.

[64] Venables, J., 1964, "The Nucleation and Propagation of Deformation Twins," J. Phys. Chem. Solids, **25**(7), pp. 693–700.

[65] Pirouz, P., 1989, "On Twinning and Polymorphic Transformations in Compound Semiconductors," Scr. Metall., **23**(3), pp. 401–406.

[66] Miura, S., Takamura, J., and Narita, N., 1968, "Orientation Dependence of Flow Stress for Twinning in Silver Crystals," Transactions of the Japan Institute of Metals, Sendai, Japan, p. 555.

[67] Meyers, M., Vöhringer, O., and Lubarda, V., 2001, "The Onset of Twinning in Metals: A Constitutive Description," Acta Mater., **49**(19), pp. 4025–4039.

[68] Fischer, F., Appel, F., and Clemens, H., 2003, "A Thermodynamical Model for the Nucleation of Mechanical Twins in TiAl," Acta Mater., **51**(5), pp. 1249–1260.

[69] Tadmor, E., and Hai, S., 2003, "A Peierls Criterion for the Onset of Deformation Twinning at a Crack Tip," J. Mech. Phys. Solids, **51**(5), pp. 765–793.

[70] Kibey, S. A., Wang, L.-L., Liu, J. B., Johnson, H. T., Sehitoglu, H., and Johnson, D. D., 2009, "Quantitative Prediction of Twinning Stress in Fcc Alloys: Application to Cu-Al," Phys. Rev. B, **79**(21), p. 214202.

[71] Ojha, A., Sehitoglu, H., Patriarca, L., and Maier, H., 2014, "Twin Migration in Fe-Based Bcc Crystals: Theory and Experiments," Philos. Mag., **94**(16), pp. 1816–1840.

[72] Joos, B., Ren, Q., and Duesbery, M., 1994, "Peierls-Nabarro Model of Dislocations in Silicon With Generalized Stacking-Fault Restoring Forces," Phys. Rev. B, **50**(9), p. 5890.

[73] Schoeck, G., 1994, "The Generalized Peierls–Nabarro Model," Philos. Mag. A, **69**(6), pp. 1085–1095.

[74] Peierls, R., 1940, "The Size of a Dislocation," Proc. Phys. Soc., **52**(1), pp. 34–37.

[75] Nabarro, F., 1947, "Dislocations in a Simple Cubic Lattice," Proc. Phys. Soc., **59**(2), p. 256.

[76] Kibey, S., Liu, J., Johnson, D., and Sehitoglu, H., 2007, "Predicting Twinning Stress in Fcc Metals: Linking Twin-Energy Pathways to Twin Nucleation," Acta Mater., **55**(20), pp. 6843–6851.

[77] Koning, M. D., Miller, R., Bulatov, V., and Abraham, F. F., 2002, "Modelling Grain-Boundary Resistance in Intergranular Dislocation Slip Transmission," Philos. Mag. A, **82**(13), pp. 2511–2527.

[78] Hirth, J. P., and Lothe, J., 1982, Theory of Dislocations, Krieger Publishing Company, Malabar, FL.

[79] Mahajan, S., and Chin, G., 1974, "The Interaction of Twins With Existing Substructure and Twins in Cobalt-Iron Alloys," Acta Metall., **22**(9), pp. 1113–1119.

[80] Li, J., 1960, "The Interaction of Parallel Edge Dislocations With a Simple Tilt Dislocation Wall," Acta Metall., **8**(5), pp. 296–311.

[81] Li, J., and Chalmers, B., 1963, "Energy of a Wall of Extended Dislocations," Acta Metall., **11**(4), pp. 243–249.

[82] Li, J. C., and Needham, C. D., 1960, "Some Elastic Properties of a Screw Dislocation Wall," J. Appl. Phys., **31**(8), pp. 1318–1330.

[83] Neumann, P., 1986, "Low Energy Dislocation Configurations: A Possible Key to the Understanding of Fatigue," Mater. Sci. Eng., **81**, pp. 465–475.

[84] Lu, L., Chen, X., Huang, X., and Lu, K., 2009, "Revealing the Maximum Strength in Nanotwinned Copper," Science, **323**(5914), pp. 607–610.

[85] Lu, L., Shen, Y., Chen, X., Qian, L., and Lu, K., 2004, "Ultrahigh Strength and High Electrical Conductivity in Copper," Science, **304**(5669), pp. 422–426.

[86] Deng, C., and Sansoz, F., 2009, "Fundamental Differences in the Plasticity of Periodically Twinned Nanowires in Au, Ag, Al, Cu, Pb, and Ni," Acta Mater., **57**(20), pp. 6090–6101.

[87] Asaro, R. J., and Suresh, S., 2005, "Mechanistic Models for the Activation Volume and Rate Sensitivity in Metals With Nanocrystalline Grains and Nano-Scale Twins," Acta Mater., **53**(12), pp. 3369–3382.

[88] Lu, L., Schwaiger, R., Shan, Z., Dao, M., Lu, K., and Suresh, S., 2005, "Nano-Sized Twins Induce High Rate Sensitivity of Flow Stress in Pure Copper," Acta Mater., **53**(7), pp. 2169–2179.

[89] Wei, Q., Cheng, S., Ramesh, K., and Ma, E., 2004, "Effect of Nanocrystalline and Ultrafine Grain Sizes on the Strain Rate Sensitivity and Activation Volume: Fcc Versus Bcc Metals," Mater. Sci. Eng. A, **381**(1), pp. 71–79.

[90] Jennings, A. T., Li, J., and Greer, J. R., 2011, "Emergence of Strain-Rate Sensitivity in Cu Nanopillars: Transition From Dislocation Multiplication to Dislocation Nucleation," Acta Mater., **59**(14), pp. 5627–5637.

[91] Lim, L., 1984, "Slip-Twin Interactions in Nickel at 573K at Large Strains," Scr. Metall., **18**(10), pp. 1139–1142.

[92] Evans, J., 1974, "Heterogeneous Shear of a Twin Boundary in α-Brass," Scr. Metall., **8**(9), pp. 1099–1103.

[93] Deng, C., and Sansoz, F., 2009, "Size-Dependent Yield Stress in Twinned Gold Nanowires Mediated by Site-Specific Surface Dislocation Emission," Appl. Phys. Lett., **95**(9), p. 091914.

[94] Ezaz, T., Sangid, M. D., and Sehitoglu, H., 2011, "Energy Barriers Associated With Slip–Twin Interactions," Philos. Mag., **91**(10), pp. 1464–1488.

[95] Wu, Z., Zhang, Y., and Srolovitz, D., 2009, "Dislocation–Twin Interaction Mechanisms for Ultrahigh Strength and Ductility in Nanotwinned Metals," Acta Mater., **57**(15), pp. 4508–4518.

[96] Hartley, C. S., and Blachon, D. L., 1978, "Reactions of Slip Dislocations at Coherent Twin Boundaries in Face-Centered-Cubic Metals," J. Appl. Phys., **49**(9), pp. 4788–4796.

[97] Lee, T., Robertson, I., and Birnbaum, H., 1990, "An In Situ Transmission Electron Microscope Deformation Study of the Slip Transfer Mechanisms in Metals," Metall. Trans. A, **21**(9), pp. 2437–2447.

[98] Kulkarni, Y., and Asaro, R. J., 2009, "Are Some Nanotwinned Fcc Metals Optimal for Strength, Ductility and Grain Stability?," Acta Mater., **57**(16), pp. 4835–4844.

[99] Müllner, P., and Solenthaler, C., 1997, "On the Effect of Deformation Twinning on Defect Densities," Mater. Sci. Eng. A, **230**(1), pp. 107–115.

[100] El Kadiri, H., and Oppedal, A., 2010, "A Crystal Plasticity Theory for Latent Hardening by Glide Twinning Through Dislocation Transmutation and Twin Accommodation Effects," J. Mech. Phys. Solids, **58**(4), pp. 613–624.

[101] Jin, Z.-H., Gumbsch, P., Albe, K., Ma, E., Lu, K., Gleiter, H., and Hahn, H., 2008, "Interactions Between Non-Screw Lattice Dislocations and Coherent Twin Boundaries in Face-Centered-Cubic Metals," Acta Mater., **56**(5), pp. 1126–1135.

[102] Mahajan, S., and Chin, G., 1973, "Twin-Slip, Twin-Twin and Slip-Twin Interactions in Co-8 wt.% Fe Alloy Single Crystals," Acta Metall., **21**(2), pp. 173–179.

[103] Alkan, S., Chowdhury, P., Sehitoglu, H., Rateick, R. G., and Maier, H. J., 2016, "Role of Nanotwins on Fatigue Crack Growth Resistance–Experiments and Theory," Int. J. Fatigue, **84**, pp. 28–39.

[104] Chowdhury, P. B., Sehitoglu, H., Rateick, R. G., and Maier, H. J., 2013, "Modeling Fatigue Crack Growth Resistance of Nanocrystalline Alloys," Acta Mater., **61**(7), pp. 2531–2547.

[105] Chowdhury, P., Sehitoglu, H., and Rateick, R., 2016, "Recent Advances in Modeling Fatigue Cracks at Microscale in the Presence of High Density Coherent Twin Interfaces," Curr. Opin. Solid State Mater. Sci., **20**(3), pp. 140–150.

[106] Zhang, R., Wang, J., Beyerlein, I., and Germann, T., 2011, "Twinning in Bcc Metals Under Shock Loading: A Challenge to Empirical Potentials," Philos. Mag. Lett., **91**(12), pp. 731–740.

[107] Shi, Z., and Singh, C. V., 2016, "Competing Twinning Mechanisms in Body-Centered Cubic Metallic Nanowires," Scr. Mater., **113**, pp. 214–217.

[108] Estrin, Y., and Mecking, H., 1984, "A Unified Phenomenological Description of Work Hardening and Creep Based on One-Parameter Models," Acta Metall., **32**(1), pp. 57–70.

[109] Jackson, P., and Basinski, Z., 1967, "Latent Hardening and the Flow Stress in Copper Single Crystals," Can. J. Phys., **45**(2), pp. 707–735.

[110] Friedel, J., 1955, "CXXX. On the Linear Work Hardening Mate of Face-Centred Cubic Single Crystals," Philos. Mag., **46**(382), pp. 1169–1186.

[111] Lomer, W., 1951, "A Dislocation Reaction in the Face-Centred Cubic Lattice," London, Edinburgh, Dublin Philos. Mag. J. Sci., **42**(334), pp. 1327–1331.

[112] Garstone, J., and Honeycombe, R., 1957, Dislocations and Mechanical Properties of Crystals, Wiley, New York, p. 391.

[113] Robertson, I. M., 1986, "Microtwin Formation in Deformed Nickel," Philos. Mag. A, **54**(6), pp. 821–835.

[114] Chowdhury, P., Canadinc, D., and Sehitoglu, H., 2017, "On Deformation Behavior of Fe-Mn Based Structural Alloys," Mater. Sci. Eng.: R: Rep., **122**, pp. 1–28.

[115] Yamakov, V., Wolf, D., Phillpot, S. R., Mukherjee, A. K., and Gleiter, H., 2002, "Dislocation Processes in the Deformation of Nanocrystalline Aluminium by Molecular-Dynamics Simulation," Nat. Mater., **1**(1), pp. 45–49.

[116] Shabib, I., and Miller, R. E., 2009, "Deformation Characteristics and Stress–Strain Response of Nanotwinned Copper Via Molecular Dynamics Simulation," Acta Mater., **57**(15), pp. 4364–4373.

[117] Li, X., Wei, Y., Lu, L., Lu, K., and Gao, H., 2010, "Dislocation Nucleation Governed Softening and Maximum Strength in Nano-Twinned Metals," Nature, **464**(7290), pp. 877–880.

[118] Zhu, T., and Gao, H., 2012, "Plastic Deformation Mechanism in Nanotwinned Metals: An Insight From Molecular Dynamics and Mechanistic Modeling," Scr. Mater., **66**(11), pp. 843–848.

[119] Chowdhury, P. B., 2011, Fatigue Crack Growth (FCG) Modeling in the Presence of Nano-Obstacles, University of Illinois at Urbana-Champaign, Urbana, IL.

[120] Chowdhury, P., Sehitoglu, H., and Rateick, R., 2017, "Damage Tolerance of Carbon-Carbon Composites in Aerospace Application," Carbon, **126**, pp. 382–393.

[121] Rice, J. R., 1992, "Dislocation Nucleation From a Crack Tip: An Analysis Based on the Peierls Concept," J. Mech. Phys. Solids, **40**(2), pp. 239–271.

[122] Rice, J. R., and Thomson, R., 1974, "Ductile Versus Brittle Behaviour of Crystals," Philos. Mag., **29**(1), pp. 73–97.

[123] deCelis, B., Argon, A. S., and Yip, S., 1983, "Molecular Dynamics Simulation of Crack Tip Processes in Alpha-Iron and Copper," J. Appl. Phys., **54**(9), pp. 4864–4878.

[124] Chowdhury, P. B., Sehitoglu, H., and Rateick, R. G., 2014, "Predicting Fatigue Resistance of Nano-Twinned Materials—Part I: Role of Cyclic Slip Irreversibility and Peierls Stress," Int. J. Fatigue, **68**, pp. 277–291.

[125] Chowdhury, P. B., Sehitoglu, H., and Rateick, R. G., 2014, "Predicting Fatigue Resistance of Nano-Twinned Materials—Part II: Effective Threshold Stress Intensity Factor Range," Int. J. Fatigue, **68**, pp. 292–301.

[126] Xie, C., Fang, Q. H., Liu, X., Guo, P. C., Chen, J. K., Zhang, M. H., Liu, Y. W., Rolfe, B., and Li, L. X., 2016, "Theoretical Study on the {1̄012} Deformation Twinning and Cracking in Coarse-Grained Magnesium Alloys," Int. J. Plast., **82**, pp. 44–61.

[127] Otsuka, K., and Wayman, C. M., 1999, *Shape Memory Materials*, Cambridge University Press, Cambridge, UK.

[128] Chowdhury, P., Patriarca, L., Ren, G., and Sehitoglu, H., 2016, "Molecular Dynamics Modeling of NiTi Superelasticity in Presence of Nanoprecipitates," Int. J. Plast., **81**, pp. 152–167.

[129] Lai, W., and Liu, B., 2000, "Lattice Stability of Some Ni-Ti Alloy Phases Versus Their Chemical Composition and Disordering," J. Phys.: Condens. Matter, **12**(5), p. L53.

[130] Chowdhury, P., and Sehitoglu, H., 2016, "Significance of Slip Propensity Determination in Shape Memory Alloys," Scr. Mater., **119**, pp. 82–87.

[131] Chowdhury, P., and Sehitoglu, H., 2017, "Deformation Physics of Shape Memory Alloys–Fundamentals at Atomistic Frontier," Prog. Mater. Sci., **88**, pp. 49–88.

[132] Mirzaeifar, R., Gall, K., Zhu, T., Yavari, A., and DesRoches, R., 2014, "Structural Transformations in NiTi Shape Memory Alloy Nanowires," J. Appl. Phys., **115**(19), p. 194307.

[133] Mutter, D., and Nielaba, P., 2013, "Simulation of the Shape Memory Effect in a NiTi Nano Model System," J. Alloys Compd., **577**(Suppl. 1), pp. S83–S87.

[134] Chowdhury, P., Ren, G., and Sehitoglu, H., 2015, "NiTi Superelasticity Via Atomistic Simulations," Philos. Mag. Lett., **95**(12), pp. 1–13.

[135] Chowdhury, P., and Sehitoglu, H., 2016, "A Revisit to Atomistic Rationale for Slip in Shape Memory Alloys," Prog. Mater. Sci., **85**, pp. 1–42.

[136] Wang, F., and Agnew, S. R., 2016, "Dislocation Transmutation by Tension Twinning in Magnesium Alloy AZ31," Int. J. Plast., **81**, pp. 63–86.

[137] El Kadiri, H., Baird, J. C., Kapil, J., Oppedal, A. L., Cherkaoui, M., and Vogel, S. C., 2013, "Flow Asymmetry and Nucleation Stresses of Twinning and Non-Basal Slip in Magnesium," Int. J. Plast., **44**, pp. 111–120.

[138] Ishii, A., Li, J., and Ogata, S., 2016, "Shuffling-Controlled Versus Strain-Controlled Deformation Twinning: The Case for HCP Mg Twin Nucleation," Int. J. Plast., **82**, pp. 32–43.

[139] Ngan, A., 1995, "A Critique on Some of the Concepts Regarding Planar Faults in Crystals," Philos. Mag. Lett., **72**(1), pp. 11–19.

[140] Zimmerman, J. A., Gao, H., and Abraham, F. F., 2000, "Generalized Stacking Fault Energies for Embedded Atom FCC Metals," Modell. Simul. Mater. Sci. Eng., **8**(2), p. 103.

[141] Kibey, S., Liu, J. B., Johnson, D. D., and Sehitoglu, H., 2006, "Generalized Planar Fault Energies and Twinning in Cu–Al Alloys," Appl. Phys. Lett., **89**(19), p. 191911.

[142] Cai, W., and Bulatov, V. V., 2004, "Mobility Laws in Dislocation Dynamics Simulations," Mater. Sci. Eng.: A, **387–389**, pp. 277–281.

[143] Devincre, B., Kubin, L., Lemarchand, C., and Madec, R., 2001, "Mesoscopic Simulations of Plastic Deformation," Mater. Sci. Eng.: A, **309–310**, pp. 211–219.

[144] Amodeo, R., and Ghoniem, N., 1990, "Dislocation Dynamics—I: A Proposed Methodology for Deformation Micromechanics," Phys. Rev. B, **41**(10), p. 6958.

[145] Kocks, U. F., Argon, A. S., and Ashby, M. F., 1975, *Thermodynamics and Kinetics of Slip*, Pergamon Press, Oxford, UK.

[146] Clayton, J. D., 2010, *Nonlinear Mechanics of Crystals*, Springer Science & Business Media, New York.